Do all leaf photosynthesis parameters of rice acclimate to elevated CO

Cai, C., Li, G., Yang, H., Yang, J., Liu, H., Struik, P. C., ... Zhu, J.

Please cite this publication as follows:

Cai, C., Li, G., Yang, H., Yang, J., Liu, H., Struik, P. C., ... Zhu, J. (2018). Do all leaf photosynthesis parameters of rice acclimate to elevated CO2, elevated temperature, and their combination, in FACE environments? Global Change Biology, 24(4), 1685-1707. https://doi.org/10.1111/gcb.13961

Received: 3 June 2017 | Accepted: 10 October 2017
DOI: 10.1111/gcb.13961

PRIMARY RESEARCH ARTICLE

WILEY Global Change Biology

Do all leaf photosynthesis parameters of rice acclimate to elevated CO_2, elevated temperature, and their combination, in FACE environments?

Chuang Cai[1] | Gang Li[1] | Hailong Yang[1] | Jiaheng Yang[1] | Hong Liu[1] | Paul C. Struik[2] | Weihong Luo[1] | Xinyou Yin[2] | Lijun Di[1] | Xuanhe Guo[1] | Wenyu Jiang[1] | Chuanfei Si[1] | Genxing Pan[3] | Jianguo Zhu[4]

[1]College of Agriculture, Nanjing Agricultural University, Nanjing, Jiangsu, China

[2]Centre for Crop Systems Analysis, Department of Plant Sciences, Wageningen University & Research, Wageningen, The Netherlands

[3]College of Resources and Environmental Sciences, Nanjing Agricultural University, Nanjing, Jiangsu, China

[4]State Key Laboratory of Soil and Sustainable Agriculture, Institute of Soil Science, Chinese Academy of Sciences, Nanjing, China

Correspondence
Weihong Luo, College of Agriculture, Nanjing Agricultural University, Nanjing, Jiangsu, China.
Email: lwh@njau.edu.cn
and
Xinyou Yin, Centre for Crop Systems Analysis, Department of Plant Sciences, Wageningen University & Research, Wageningen, The Netherlands.
Email: xinyou.yin@wur.nl

Funding information
Ministry of Agriculture of the People's Republic of China, Grant/Award Number: 200903003; National Natural Science Foundation of China, Grant/Award Number: 31261140364, 31400372; State Administration of Foreign Experts Affairs of the People's Republic of China and Ministry of Education of the People's Republic of China, Grant/Award Number: B16026; Netherlands Organisation for Scientific Research

Abstract

Leaf photosynthesis of crops acclimates to elevated CO_2 and temperature, but studies quantifying responses of leaf photosynthetic parameters to combined CO_2 and temperature increases under field conditions are scarce. We measured leaf photosynthesis of rice cultivars Changyou 5 and Nanjing 9108 grown in two free-air CO_2 enrichment (FACE) systems, respectively, installed in paddy fields. Each FACE system had four combinations of two levels of CO_2 (ambient and enriched) and two levels of canopy temperature (no warming and warmed by 1.0–2.0°C). Parameters of the C_3 photosynthesis model of Farquhar, von Caemmerer and Berry (the FvCB model), and of a stomatal conductance (g_s) model were estimated for the four conditions. Most photosynthetic parameters acclimated to elevated CO_2, elevated temperature, and their combination. The combination of elevated CO_2 and temperature changed the functional relationships between biochemical parameters and leaf nitrogen content for Changyou 5. The g_s model significantly underestimated g_s under the combination of elevated CO_2 and temperature by 19% for Changyou 5 and by 10% for Nanjing 9108 if no acclimation was assumed. However, our further analysis applying the coupled g_s–FvCB model to an independent, previously published FACE experiment showed that including such an acclimation response of g_s hardly improved prediction of leaf photosynthesis under the four combinations of CO_2 and temperature. Therefore, the typical procedure that crop models using the FvCB and g_s models are parameterized from plants grown under current ambient conditions may not result in critical errors in projecting productivity of paddy rice under future global change.

KEYWORDS
climate change, free-air CO_2 enrichment, leaf nitrogen content, mesophyll conductance, *Oryza sativa* L., photosynthesis model, stomatal conductance

1 | INTRODUCTION

The atmospheric CO_2 and global mean surface air temperature are rising. Crops are sensitive to these changes, but may adjust photosynthetic capacity in response to prolonged changes in air temperature and CO_2 concentration over the growing season (Adachi et al., 2014; Alonso, Pérez, & Martínez-Carrasco, 2009; Borjigidai et al., 2006; Pozo, Pérez, Morcuende, Alonso, & Martínez-Carrasco, 2005). However, many studies on predicting crop yield under future climate change using current crop models did not take these acclimation responses of photosynthetic capacity into account (Asseng et al., 2004; Kim, Ko, Kang, & Tenhunen, 2013; Li et al., 2014), partly because these responses are poorly understood and inadequately quantified.

Acclimation responses in photosynthesis and respiration to changes in atmospheric CO_2 concentration and temperature have been explored as major stimuli eliciting adjustments in plant photosynthetic capacity (Ainsworth & Long, 2005; Alonso et al., 2009). Under a prolonged increase in CO_2 concentration, photosynthesis is often down-regulated, in many instances quantified by the decrease in two biochemical parameters of the model of Farquhar, von Caemmerer, and Berry (1980, the FvCB model): the maximum rates of electron transport (J_{max}) and of carboxylation by Rubisco (V_{cmax}) (Drake, González-Meler, & Long, 1997; Long, Ainsworth, Rogers, & Ort, 2004; Pérez, Morcuende, Martin del Molino, & Martinez-Carrasco, 2005). A prolonged increase in temperature also results in decreases in the temperature sensitivity of leaf respiration in the light or called day respiration (R_d) (Atkin, Scheurwater, & Pons, 2006; Chi et al., 2013; Crous et al., 2011).

These biochemical parameters J_{max}, V_{cmax} and R_d are also influenced by the physiological status of a leaf, for example they are linearly correlated with the amount of nitrogen (N) per unit leaf area (e.g. Harley, Thomas, Reynolds, & Strain, 1992). The fact that photosynthesis is not strongly enhanced by long-term elevated CO_2 may be associated with the inability of plants to acquire more nitrogen, resulting in lower leaf nitrogen content in plants grown under CO_2 enrichment (Drake et al., 1997; Luo et al., 2004; Peterson et al., 1999). Yin (2013) found that elevated CO_2 did not change the linear relationship between V_{cmax} or J_{max} and leaf nitrogen content.

The CO_2 diffusion from the atmosphere to the sub-stomatal cavity (reflected in stomatal conductance, g_s) and the diffusion from intercellular airspace within a leaf to the sites of carboxylation within chloroplasts (reflected in mesophyll conductance, g_m) may also limit leaf photosynthesis. Some studies explored acclimation responses of g_s to elevated CO_2 and elevated temperature, but with inconsistent results (Bunce, 2000, 2004; Leakey, Bernacchi, et al., 2006; Pozo et al., 2005). Only a few studies showed that elevated temperature and the combination of elevated CO_2 and elevated temperature caused strong acclimation of g_s in a controlled environment. Leakey, Bernacchi, et al. (2006) suggested the acclimation extent and nature of g_s, like for photosynthesis rate, may differ between FACE (free-air CO_2 enrichment) and growth chamber studies. The responses of g_m to short-term changes in CO_2 level are inconsistent (Flexas et al., 2012, 2014). Bernacchi, Portis, Nakano, von Caemmerer, and Long (2002) used a peaked Arrhenius function to parameterize short-term responses of g_m to temperature, but such responses differ greatly among species (von Caemmerer & Evans, 2015). There are no general trends for g_m in plants grown under elevated CO_2 and elevated temperature (Chi et al., 2013; Dillaway & Kruger, 2010; Flexas, Ribas-Carbó, Diaz-Espejo, Galmés, & Medrano, 2008; Flexas et al., 2012; Yamori, Noguchi, Hanba, & Terashima, 2006), and no studies have parameterized the temperature response of g_m under combined elevated CO_2 and elevated temperature. Therefore, it is necessary to explore any acclimation responses of g_s and g_m to the combinations of elevated CO_2 and elevated temperature in FACE experiments.

Field-grown plants, exposed to natural diurnal, seasonal and year-to-year fluctuations in leaf temperature in a FACE system, would better suit for studies on plant responses to atmospheric CO_2 concentration and temperature with minimal artefacts (Long et al., 2004). Some studies found diurnal and seasonal variation in the magnitude of the decrease in g_s for plants grown under elevated CO_2 in FACE (Bernacchi et al., 2006; Leakey, Bernacchi, Ort, & Long, 2006; Shimono et al., 2010). Seasonal changes in growth temperature also affect the temperature dependence of biochemical parameters (Kattge & Knorr, 2007; Yamaguchi, Nakaji, Hiura, & Hikosaka, 2016; Yamori, Noguchi, & Terashima, 2005; Zhu, Li, Su, Lu, & Huang, 2011). Kattge and Knorr (2007) analyzed data from 36 plant species to quantify the temperature dependence of J_{max} and V_{cmax} with their prevailing growth temperature and found that the optimum temperature of J_{max} and V_{cmax} increased with increasing growth temperature. Photosynthesis parameters estimated from gas exchange data obtained from in situ measurements that cover diurnal and seasonal changes will be able to assess the "actual" responses of leaves in the field (Kosugi, Shibata, & Kobashi, 2003; Zhu et al., 2011). However, so far, few studies investigated seasonal acclimation of photosynthesis parameters to combined elevated CO_2 and elevated temperature.

The primary objective of this study is to analyse seasonal acclimation of leaf photosynthesis and photosynthetic parameters to elevated CO_2 and elevated temperature and their combination under field conditions, and to quantify the relationships between the photosynthetic capacity and leaf nitrogen content. Photosynthesis was therefore measured on leaves of two rice cultivars, each grown under a specific FACE set-up. We also aim to quantify the error of prediction by the prevailing crop models where parameters are typically obtained from plants grown under ambient conditions, i.e. assuming no acclimation response to elevated CO_2 and temperature in the models.

2 | MATERIALS AND METHODS

2.1 | FACE systems

Field experiments were conducted in two FACE systems, identified here as FACE 1 and FACE 2.

FACE 1 was established in Kangbo village (31°30′N, 120°33′E), Guli Township, Changshu Municipality, Jiangsu, China, in 2010. Mean annual temperature and precipitation at this site in 2004–2013 were 16°C and 1,100–1,200 mm, respectively. Details of the rationale, design, operation, and performance of the FACE system are similar to those described by Cai et al. (2016). The FACE system had twelve octagonal plots located in different sites with similar soils and agronomic histories, each measuring ca. 50 m^2. The CO_2 exposure system was designed following the rationale as described by Okada, Lieffering, Nakamura, Kim, and Kobayashi (2001). Sixteen Li-

820 CO_2 sensors (Li-COR Inc., Lincoln, NE, USA) per plot were installed above the canopy, evenly distributed in two concentric circles, to automatically control the CO_2 pumping. The consistency of the CO_2 concentration within the ring was controlled by automatic adjustment to wind direction and velocity. The infrared heating facilities were designed based on the principles described by Kimball et al. (2008). The facility consisted of 12 infrared heaters (2,000 W, 240 V, 1.65 m long × 0.14 m wide; HS-2420; Kalglo Electronics Co., Inc., Bethlehem, PA, USA). The heaters were adjusted weekly at 1.2 m above the top of the canopy during the growth cycle. Canopy temperature was sensed using six infrared thermometers (Model SI-121; Apogee Instruments Inc, Logan, USA), arranged inside the experimental plot in a hexagonal array. There were four treatments in a block split-plot design: (1) in CT, ambient conditions were maintained (control); (2) in C+T, the target atmospheric CO_2 was up to 500 μmol/mol; (3) in CT+, the canopy temperature was warmed by 1.5–2.0°C, and (4) in C+T+, CO_2 enrichment was combined with warming. The treatment levels for CO_2 enrichment and warming were defined for climate conditions of a target year around 2040.

FACE 2 was initially established in Xiaoji Township (32°35′N, 119°42′E), Jiangdu Municipality, Jiangsu, China, in 2004, for elevating CO_2 only. Mean annual temperature and precipitation at this site in 2004–2013 were 16°C and 1,000–1,100 mm, respectively. The FACE system had six octagonal plots located in different sites with similar soils and agronomic histories, each measuring ca. 80 m^2. The CO_2 exposure system was also designed according to Okada et al. (2001). The CO_2 exposure system and its performance have been described in detail by Liu et al. (2002) and Han, Liu, Zhu, Okada, and Yoshimoto (2002). The temperature control system was introduced in 2014; it is described in Jing, Lai, Wang, Yang, and Wang (2016), Jing, Wang, et al. (2016). In brief, the temperature control system contained seven subplots (2.7 m long × 0.76 m width each), which were heated by sixteen copper pipes installed at the top of the canopy (Figure 1a). Heat radiation emitted from the running hot water in the copper pipes increased the air temperature around nearby plants. Elevated canopy temperature by ca. 1°C was achieved by coordinated work of a temperature sensor and a computer feedback system that controlled the speed of the running hot water. The temperature of hot water was kept in the range of 60–70°C. The velocity of the hot water flow was changed, taking into account the wind speed over the canopy. The copper pipes were adjusted weekly so as to maintain their height at the top of the canopy during the growth cycle. Canopy temperature was sensed automatically using an infrared thermometer (Model SI-131; Apogee Instruments Inc) with a sensing area ca. 0.05 m^2 at the centre of the 4th subplot (Figure 1a). Canopy thermal image of the overall area in each heated subplot was manually scanned using FLIR Systems (Model T630sc, Stockholm, Sweden) before heading. The thermal image showed that the temperature control system created a quite uniform canopy temperature within the heated subplots (Figure 1b). Canopy temperature of the infrared thermometer target area (El1) was only 0.2°C lower than the average canopy temperature (derived from the thermal image) of the overall area (Ar1) in each heated subplot (Figure 1b). There were four treatments: (1) in CT, ambient conditions were maintained (control); (2) in C+T, the target atmospheric CO_2 was maintained at about 200 μmol/mol above the ambient level; (3) in CT+, the daytime canopy temperature was warmed by 1.0°C, and (4) in C+T+, CO_2 enrichment was combined with warming (Table 1).

2.2 | FACE experiments

The experiment in FACE 1 was conducted in 2016 using local rice cultivar Changyou 5. Seedlings of japonica cv. Changyou 5 grown under ambient air were manually transplanted at a density of 3 seedlings per hill into all plots on 25 June. Spacing of hills was 15.3 cm × 25.4 cm (equivalent to 25.7 hills/m^2; 77.1 plants/m^2). The CO_2 and temperature treatments were carried out from 3 July through to harvest. We sprayed pure CO_2 during day time and increased canopy temperature both day and night. Detailed information on the increases in canopy temperature realized under CT+ and C+T+ and the average daytime increase in CO_2 concentration realized under C+T and C+T+ is provided in Table 1.

FACE 2 experiment was implemented also in 2016. Seedlings of japonica cv. Nanjing 9108 grown under ambient air were manually transplanted at a density of 2 seedlings per hill into all plots on 21 June. Spacing of hills was 16.7 cm × 25.0 cm (equivalent to 24.0 hills/m^2; 48.0 plants/m^2). The CO_2 and temperature treatments

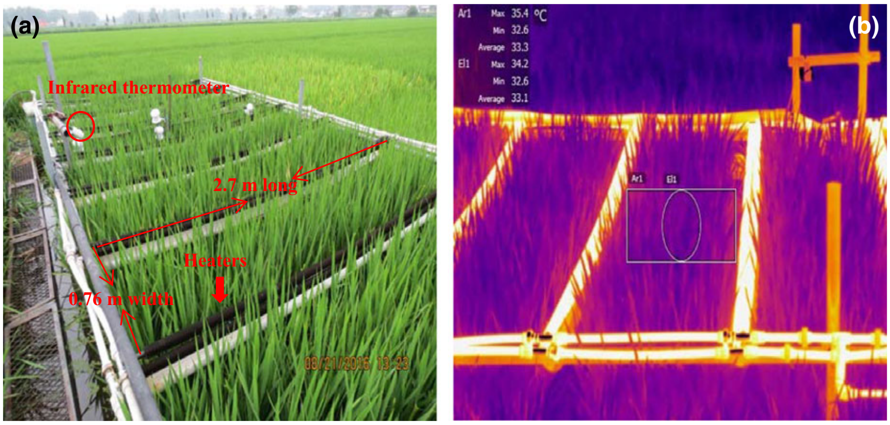

FIGURE 1 The FACE 2 experiment: (a) picture of the temperature control facility; (b) thermal image of the warming pattern produced by the heaters obtained around noon on 12 August 2016 with the heaters fully on (Ar1 stands for overall area; El1 stands for target area sensed by infrared thermometer) [Colour figure can be viewed at wileyonlinelibrary.com]

TABLE 1 Summary of the environmental conditions in FACE 1 experiment and FACE 2 experiment

	2016		2014^{a}
	FACE 1 experiment	**FACE 2 experiment**	**FACE 1 experiment**
CO_2 concentration increment relative to CT (μmol/mol)			
C+T	110 (23)	199 (15)	109 (35)
C+T+	104 (25)	199 (15)	82 (29)
Canopy temperature^{b} increment relative to CT (°C)			
CT+	1.7 (0.1); 2.1 (0.2)	1.0 (0.0); 0.1 (0.0)	2.0 (1.0); 2.3 (1.4)
C+T+	1.7 (0.2); 2.0 (0.3)	1.4 (0.0); 0.0 (0.0)	1.9 (0.9); 1.7 (1.1)
Mean daily air temperature (°C)	26.3 (3.7)	25.0 (3.2)	24.2 (3.4)
Mean daily global radiation (MJ m^{-2} day^{-1})	12.7 (0.5)	12.2 (0.5)	8.3 (0.3)
Basal N applied (g/m^2)^{c}	6.9 (−3)	9.0 (−1)	6.9 (0)
Top-dressed N (g/m^2)^{c}	6.0 (12) 5.2 (34)	6.8 (7) 6.8 (35)	6.0 (29) 5.2 (46)

CT, C+T, CT+ and C+T+ stand for ambient condition, elevated CO_2, elevated temperature, and the combination of elevated CO_2 and elevated temperature, respectively.

Data in the table represent seasonal average values (SD between the daily values in brackets) for the average daytime increase in CO_2 concentration, average daily increase in daytime (the first pair of data), and night-time (the second pair of data) canopy temperature, daily mean air temperature, mean daily solar radiation during the whole cycle, and level of nitrogen (N) application for each FACE experiment (for meaning of values in brackets see below).

[a] Data for 2014 in the FACE 1 experiment are from Cai et al. (2016) and merely used here for model validation (see the text).

[b] Temperature at the top of rice canopies was sensed by infrared thermometers.

[c] Values in brackets refer to the time of N application, expressed in days after transplanting. All nitrogen was applied before the stem-elongating stage for all experiments.

in the FACE system (Table 1) were carried out from 28 June through to harvest, and the treatment time each day for both CO_2 and temperature was from sunrise to sunset.

In both FACE systems, all net plots were surrounded by at least three rows of border plants treated in the same way as the plants within the net plots. Standard cultivation practices for paddy rice were followed in all experimental plots. Daily weather data during the growing season for maximal and minimal air temperatures, global radiation, relative humidity (RH), wind speed and precipitation for both experiments are shown in Fig. S1.

2.3 | Gas exchange and chlorophyll fluorescence measurement

We used the LI-Cor 6400XT Portable Photosynthesis System (Li-Cor BioScience, Lincoln, NE, USA) to simultaneously measure gas exchange and chlorophyll fluorescence. Measurements were conducted at three stages, i.e. at the onset of stem elongation, at heading, and during the grain-filling stage (27 and 33 days after heading for cvs Changyou 5 and Nanjing 9108, respectively), and were replicated using three youngest fully expanded leaves (which are flag leaves for measurements at heading and grain-filling stages) in each treatment and each stage.

Light and CO_2 response curves were measured on the same leaves, primarily under 21% O_2 conditions. For light response curves, prior to measurements, leaves were placed in the cuvette at incident irradiance (I_{inc}) of 2,000 μmol photons m^{-2} s^{-1}. Ten minutes later, I_{inc} in the leaf cuvette was controlled in a decreasing series of 1,500, 1,000, 800, 500, 200, 100, 50, 20 and 0 μmol photons m^{-2} s^{-1} (6 min per I_{inc} step, according to pre-measurements for the time to reach a steady-state), while keeping ambient CO_2 level (C_a) at 380 μmol/mol for all treatments for the two rice cultivars. For each CO_2 response curve, the C_a steps were: 380, 200, 100, 50, 380 (two times), 500 (for Changyou 5) or 580 (for Nanjing 9108), 1,000, 1,500 and 2,000 μmol/mol (5 min per step) under CT and CT+; 500 (for Changyou 5) or 580 (for Nanjing 9108), 380, 200, 100, 50, 500 (two times, for Changyou 5) or 580 (two times, for Nanjing 9108), 1,000, 1,500 and 2,000 μmol/mol (5 min per step) under C+T and C+T+; while keeping incident irradiance (I_{inc}) at 2,000 μmol m^{-2} s^{-1}.

Light and CO_2 responses curves of photosynthesis of two rice cultivars were made at four set-point leaf temperatures (29, 33, 36 and 39°C at stem-elongating stage; 25, 29, 33 and 39°C at heading stage; and 25, 29, 33 and 36°C at grain-filling stage). Flow rate for all measurements was 500 μmol/s. Leaf-to-air vapour pressure difference increased with leaf temperature, but was always within the range of 0.5–3.0 kPa to prevent stomatal closure (Bernacchi, Singsaas, Pimentel, Portis, & Long, 2001). As the leaf temperature control capacity was limited (with ±6°C) with the setup of the LI-6400XT system, response curves at low leaf temperature were measured in the morning and those at high leaf temperature were measured around noon, assuming that the observed responses in the biochemical parameters resulted mainly from changes in temperature rather than changes in time of day (Luo et al., 2011; Way & Sage, 2008).

At each light or CO_2 step during the measurements, the steady-state fluorescence (F_s) was measured. The maximum fluorescence (F_m') was obtained from multiphase flashes: the flash intensity was ~8,000 μmol m^{-2} s^{-1} during phase 1 for a duration of 300 ms, was attenuated by 35% during phase 2 of ~300 ms, and was back to ~8,000 μmol m^{-2} s^{-1} for phase 3 of 300 ms. The intercept of the linear regression of fluorescence yields against the inverse of the flash intensity during phase 2 gives the estimate of F_m' (Loriaux et al., 2013). The operating photochemical efficiency of photosystem II (Φ_2) was calculated as: $\Phi_2 = 1 - F_s/F_m'$ (Genty, Briantais, & Baker, 1989).

To properly estimate photosynthetic parameters, we also conducted gas exchange and chlorophyll fluorescence measurements at low oxygen using a gas blend of 2% O_2, 98% N_2 and pure CO_2 in the leaf chamber at each stage for Changyou 5 and Nanjing 9108. With 2% O_2, only the first half of the light response curves was measured: I_{inc} was increased in the order of 20, 50, 100, 150 and

200 μmol m^{-2} s^{-1}, while keeping C_a at 1,000 μmol/mol, to ensure that data used for calibration (see later) were collected within the e$^-$ transport limited range of non-photorespiratory conditions.

All CO_2 exchange rates were corrected for CO_2 leakage into and out of the leaf cuvette, based on measurements at specific temperatures using the same flow rate on boiled leaves across a range of CO_2 levels, and intercellular CO_2 levels (C_i) were then re-calculated.

2.4 | SPAD value, leaf mass and nitrogen content per unit area

SPAD value was measured using a chlorophyll meter (SPAD-502, Minolta Camera Co., Japan) on leaves of cv. Changyou 5 and Nanjing 9108, before they were used for photosynthesis measurements, at each stage. For cv. Changyou 5, the leaves were then cut, used to measure leaf area with an area meter (Li-3100; Li-Cor Inc., Lincoln, NE, USA), and then oven-dried at 105°C for 30 min, and subsequently at 80°C to constant weight and weighed. Leaf mass per area (LMA, g/m^2) was calculated thereof. The leaf nitrogen concentration was measured using the Kjeldahl digestion method. From these data, nitrogen content per leaf area (N_a, g/m^2) was calculated.

2.5 | Estimation of parameters of a biochemical model of photosynthesis

The FvCB model predicts A_n (μmol CO_2 m^{-2} s^{-1}) as the minimum of two rates, the Rubisco carboxylation-limited rate (A_c) and the RuBP regeneration- or electron transport-limited rate (A_j):

$$A_n = \min\left(A_c,\ A_j\right) \tag{1}$$

$$A_c = \frac{(C_c - \Gamma_*)V_{cmax}}{C_c + K_{mC}(1 + O/K_{mO})} - R_d \tag{2}$$

$$A_j = \frac{(C_c - \Gamma_*)J}{4(C_c + 2\Gamma_*)} - R_d \tag{3}$$

where C_c (μbar) and O (mbar) are the chloroplast partial pressures of CO_2 and O_2, respectively, K_{mC} (μbar) and K_{mO} (mbar) are the Michaelis-Menten coefficients of Rubisco for CO_2 and O_2, respectively, Γ_* (μbar) is the CO_2 compensation point in the absence of R_d (day respiration, μmol CO_2 m^{-2} s^{-1}), and J (μmol e$^-$ m^{-2} s^{-1}) is the photosystem II electron transport rate used for CO_2 fixation and photorespiration.

The calculation of A_c or A_j in the FvCB model requires C_c, which is generally unknown beforehand. We, therefore, first used our chlorophyll fluorescence data to estimate A_j-related model parameters, as described by Yin et al. (2009). To convert fluorescence-based data on Φ_2 into electron transport rate J, a calibration needs to be made. This was done by linear regression plot of A_j against ($I_{inc}\Phi_2/4$), using data of the electron-transport-limited range of the $A_n - I_{inc}$ curve under non-photorespiratory conditions (i.e. 2% O_2 combined with 1,000 μmol/mol C_a; see above). The slope s of this linear regression was used as a calibration factor to calculate values of electron transport rate under all conditions: $J = sI_{inc}\Phi_2$ (Yin et al., 2009). The obtained J was then fitted to the equation:

$$J = \frac{\kappa_{2LL}I_{inc} + J_{max} - \sqrt{(\kappa_{2LL}I_{inc} + J_{max})^2 - 4\theta J_{max}\kappa_{2LL}I_{inc}}}{2\theta} \tag{4}$$

where J_{max} (μmol e$^-$ m^{-2} s^{-1}) is the asymptotic maximum value of J when I_{inc} approaches to saturating light levels, θ is a dimensionless convexity factor for the response of J to I_{inc}, and κ_{2LL} (mol e$^-$ mol^{-1} photons) is the efficiency of converting I_{inc} into J at limiting light levels (Yin & Struik, 2009a; Yin et al., 2009). κ_{2LL} was calculated as:

$$\kappa_{2LL} = s\Phi_{2LL} \tag{5}$$

where Φ_{2LL} (mol e$^-$ mol^{-1} photons) is Φ_2 at the strictly limiting light level and could be estimated as the linear intercept of Φ_2 against I_{inc}, using data of $I_{inc} < 200$ μmol m^{-2} s^{-1} under photorespiratory conditions. We assumed θ to be constant (0.8), according to Yin and Struik (2015), and this value of θ also allows Equation (4) to have a similar curvature to the quadratic hyperbolic equation as used by Harley et al. (1992). We then used estimated κ_{2LL} and constant θ as an input to estimate J_{max} for each light response curve by fitting the data on J to Equation (4).

In principle, the parameter R_d could be estimated as the intercept of the above-mentioned linear regression of A_j against ($I_{inc}\Phi_2/4$) under non-photorespiratory conditions (Yin, Sun, Struik, & Gu, 2011; Yin et al., 2009). With J and R_d calculated, we estimated the value of g_m assuming that g_m was constant across the entire light and CO_2 response curves. Whether or not g_m is constant across light or CO_2 levels is a matter of debate; but our assumption allows to identify whether there is any difference among the four treatments in the actual average g_m. Therefore, we used the NRH-A method (Yin & Struik, 2009b) to estimate the value of g_m as constant, by fitting the following non-rectangular hyperbolic (NRH) equation for the A_j part of the C_i-based FvCB model:

$$A_j = 0.5\left\{x_1 - R_d + g_m(C_i + x_2) - \sqrt{\begin{matrix}[x_1 - R_d + g_m(C_i + x_2)]^2 - \\ 4g_m[(C_i - \Gamma_*)x_1 - R_d(C_i + x_2)]\end{matrix}}\right\} \tag{6}$$

where $x_1 = J/4$ and $x_2 = 2\Gamma_*$. We used data obtained from high C_i of CO_2 response curves and low I_{inc} levels of light response curves at 21% O_2. The comparative advantages of this method over the conventional variable-J method, and the choice of data for estimating g_m were discussed by Yin and Struik (2009b).

Equation (6) can also be applied to calculate A_c by replacing:

$$x_1 = V_{cmax} \text{ and } x_2 = K_{mC}(1 + O/K_{mO}) \tag{7}$$

We then estimated V_{cmax} by fitting the combined Equations 1, 6 and 7 to full light-response and CO_2-response curves using the already estimated J_{max}, κ_{2LL}, R_d and g_m as input.

2.6 | The temperature responses of photosynthetic parameters

Based on literature, the temperature responses of R_d, and of Rubisco kinetic properties (Γ_*, K_{mC}, K_{mO} and V_{cmax}) were described using an

Arrhenius function (Equation 8), and the temperature responses of $J_{\max}$ and of mesophyll conductance (g_m) were explored using a peaked Arrhenius function (Equation 9), normalized with respect to their values at 25°C:

$$X = X_{25}\exp\left[\frac{E_x(T-25)}{298R(T+273)}\right] \tag{8}$$

$$X = X_{25}\exp\left[\frac{E_x(T-25)}{298R(T+273)}\right]\left[\frac{1+\exp\left(\frac{298S_x-D_x}{298R}\right)}{1+\exp\left(\frac{(T+273)S_x-D_x}{R(T+273)}\right)}\right] \tag{9}$$

where T is the leaf temperature (°C), X_{25} is the value of each parameter at 25°C (R_{d25}, Γ_{*25}, $K_{mC25,}$ K_{mO25}, g_{m25}, V_{cmax25} and J_{max25}), E_x is the activation energy of each parameter (E_{Rd}, $E_{\Gamma*}$, E_{KmC}, E_{KmO}, E_{Vcmax}, E_{Jmax}, and E_{gm}; in J/mol), D_x is the deactivation energy for $J_{\max}$ and g_m (D_{Jmax} and D_{gm} in J/mol), S_x is the entropy term for $J_{\max}$ and g_m (S_{Jmax} and S_{gm} in J K^{-1} mol^{-1}), R is the universal gas constant (=8.314 J K^{-1} mol^{-1}). Rubisco kinetic properties are generally assumed constant among C_3 species (von Caemmerer, Farquhar, & Berry, 2009), and we adopted the values of Bernacchi et al. (2002) for Γ_{*25}, K_{mC25}, K_{mO25}, $E_{\Gamma*}$, E_{KmC}, and E_{KmO}. We found that Equation (9) was overparameterized for our data, as often observed in literature (Dreyer, Le Roux, Montpied, Daudet, & Masson, 2001; Li et al., 2012; Medlyn, Dreyer, et al., 2002); therefore, S_{Jmax}, S_{gm} and D_{gm} were fixed at 650 J K^{-1} mol^{-1} (Harley et al., 1992), 1,400 J K^{-1} mol^{-1} (Bernacchi et al., 2002) and 437,400 J/mol (Bernacchi et al., 2002), respectively.

The optimum temperature ($T_{opt,x}$) for $J_{\max}$ or g_m as predicted by Equation (9) is given by the following equation (Farquhar et al., 1980; Medlyn, Dreyer, et al., 2002):

$$T_{\text{opt},\,x} = \frac{D_x}{S_x - R\ln\left(\frac{E_x}{D_x-E_x}\right)} - 273 \tag{10}$$

We found that κ_{2LL} also depended on temperature, and fitted its temperature response using the normal distribution-alike equation (June, Evans, & Farquhar, 2004);

$$\kappa_{2LL} = \kappa_{2LL_{\max}}\exp\left[-\left(\frac{T-T_{\text{opt}}}{\Omega}\right)^2\right] \tag{11}$$

where κ_{2LLmax} is the maximal value of κ_{2LL}, T_{opt} is the optimum leaf temperature at which κ_{2LLmax} is obtained, and Ω describes the width of the response curve, defined as the difference between T_{opt} and the temperature at which κ_{2LL} falls to e^{-1} of κ_{2LLmax}.

2.7 | The relationships between photosynthetic biochemical parameters and leaf nitrogen content

The values of R_{d25}, J_{max25}, and V_{cmax25}, are known to linearly relate to leaf nitrogen content (N_a), with a clear base leaf nitrogen, N_b, at or below which values of these parameters become zero (Braune, Müller, & Diepenbrock, 2009; Harley et al., 1992; Hirose, Ackerly, Traw, Ramseirer, & Bazz, 1997; Müller, Wernecke, & Diepenbrock, 2005; Yin et al., 2009). g_{m25} is known to linearly scale with the photosynthetic capacity of leaves (Flexas et al., 2008). So, these parameters can be quantified by similar relationships:

$$R_{d25} = X_{Rd}(N_a - N_b) \tag{12}$$

$$J_{max25} = X_{Jmax}(N_a - N_b) \tag{13}$$

$$V_{cmax25} = X_{Vcmax}(N_a - N_b) \tag{14}$$

$$g_{m25} = X_{gm}(N_a - N_b) \tag{15}$$

where X_{Rd} (μmol CO_2 g^{-1} N s^{-1}), X_{Jmax} (μmol e^- g^{-1} N s^{-1}), X_{Vcmax} (μmol CO_2 g^{-1} N s^{-1}), and X_{gm} (mol g^{-1} N s^{-1}) are the slopes for R_{d25}, J_{max25}, V_{cmax25}, and g_{m25}, respectively. Parameter κ_{2LL} also depends on N_a, but without a clear N_b (Yin et al., 2009), and it is described here empirically as:

$$\kappa_{2LLmax} = X_{\kappa 2LL}N_a + k \tag{16}$$

where $X_{\kappa 2LL}$ and k are the slope and the intercept, respectively, of the linear regression.

2.8 | The BWB-Leuning-Yin model for stomatal conductance and its parameterization

A widely used model for g_s was initially developed by Ball, Woodrow, and Berry (1987), then extended by Leuning (1995) and Yin and Struik (2009a)—which Li et al. (2012) called the BWB-Leuning-Yin model. To explore any acclimation responses of g_s in rice to elevated CO_2 and temperature, we used the version of the BWB-Leuning-Yin model (Yin & Struik, 2009a):

$$g_s = g_0 + \frac{A+R_d}{C_i - C_{i*}}f_{\text{vpd}} \tag{17}$$

where g_0 is the residual stomatal conductance if I_{inc} approaches zero, C_i is the intercellular CO_2 concentration, C_{i*} is C_i-based CO_2 compensation point in the absence of R_d, which can be estimated as $C_{i*} = \Gamma_* - R_d/g_m$, and the effect of leaf-to-air vapour pressure difference (VPD) on g_s, f_{vpd}, is calculated according to Yin and Struik (2009a).

$$f_{\text{vpd}} = \frac{1}{1/(a_1 - b_1\text{VPD}) - 1} \tag{18}$$

where a_1 and b_1 are empirical coefficients, approximately reflecting the ratio of C_i to C_a for vapour saturated air and the decreasing slope of this ratio with increasing VPD, respectively, if g_0 approaches to zero. Combining Equations 17 and 18, we used the measured g_s, A_n, C_i and VPD at each stage to estimate g_0, a_1 and b_1. For that, measured stomatal conductance for water vapour transfer was divided by a factor 1.6 to convert it to g_s for CO_2 transfer that is required for Equation (17).

2.9 | Statistical and model analyses

Data from two rice cultivars tested were analyzed by Equations 2–9 and 11–18 with the GAUSS method in PROC NLIN of SAS (SAS Institute Inc., Cary, NC, USA). Estimated parameter values for C+T, CT+ and C+T+ treatments were compared with the value of the same parameter obtained for the control treatment CT, using a statistical F test.

Estimated parameters were then used to predict A_n (using the C_i-based FvCB model incorporating nitrogen-based functional relationships Equations 12–16) or g_s (using the BWB-Leuning-Yin model).

Two sets of prediction were compared, i.e. predictions using the treatment-specific parameters (namely assuming acclimation to growth environmental variables) vs predictions using the CT-treatment parameters (namely assuming no acclimation as by the current models where the model parameters are typically estimated from measurements on plants grown under present atmospheric conditions). Any significance in the difference between the two sets of predictions would determine the necessity to take into account acclimations in the prediction models for assessing the impact of climate change on crop growth.

We were particularly interested in assessing model predictability of A_n for an independent data set. To that end, we used the data from our previous experiment (Cai et al., 2016), which was conducted in 2014 using the FACE 1 system described here for the same cv. Changyou 5 (Table 1). Only light responses for the ambient O_2 levels were measured in that study, using uncontrolled in-situ temperature (Cai et al., 2016). To assess the impact of altered g_s parameters on predicted net photosynthesis rates A_n of Changyou 5 in 2014, we used the coupled FvCB and BWB-Leuning-Yin model using C_a and parameter values estimated here for this cultivar as input (Yin & Struik, 2009a). The coupled model is complex and has the form of a cubic polynomial, and the solution to this cubic polynomial model can be found in Yin and Struik (2009a).

Goodness of all the above predictions was assessed using the r^2 of linear regression, as well as the relative root mean squared error rRMSE (=RMSE/mean of the measured values), between predicted and measured values.

3 | RESULTS

3.1 | Photosynthesis and stomatal conductance in response to elevated CO_2 and temperature in FACE

Light and CO_2 response curves of photosynthesis of cv. Changyou 5 in the FACE 1 experiment and of cv. Nanjing 9108 in the FACE 2 experiment were assessed at four different leaf temperatures (Figures 2, 3 and S2–S5) at stem-elongating stage, heading stage and grain-filling stage of crops grown under all combinations of normal or elevated CO_2 and normal or elevated temperature. Examples of $A_n - I_{inc}$ curves (Figure 2), $A_n - C_i$ curves (Figure 3) and $g_s - I_{inc}$ curves (Figure 4) at a leaf temperature of 33°C for crops grown under the four treatments at the three stages for cv. Changyou 5 in the FACE 1 experiment and cv. Nanjing 9108 in the FACE 2 experiment are shown.

For Changyou 5 in the FACE 1 experiment, measurements at a leaf temperature of 33°C showed that compared with CT, C+T

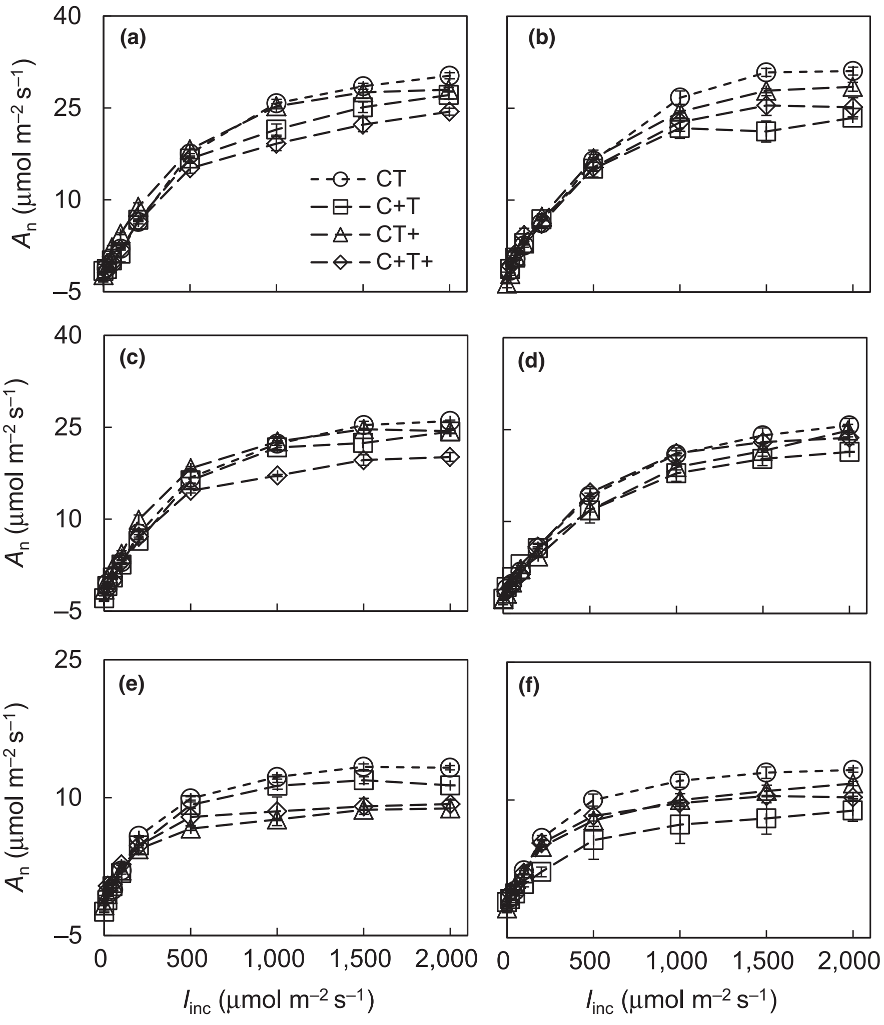

FIGURE 2 Examples of $A_n - I_{inc}$ curves at C_a of 380 μmol/mol and leaf temperature of 33°C under ambient conditions (circles, CT), elevated CO_2 (squares, C+T), elevated temperature (triangles, CT+), and a combination of elevated CO_2 and elevated temperature (diamonds, C+T+) for cv. Changyou 5 (a, c, e) in the FACE 1 experiment and cv. Nanjing 9108 (b, d, f) in the FACE 2 experiment during the stem-elongating stage (a, b), heading stage (c, d), and grain-filling stage (e, f). Each data point represents the mean value of three replications (with bars for ± standard errors of the mean)

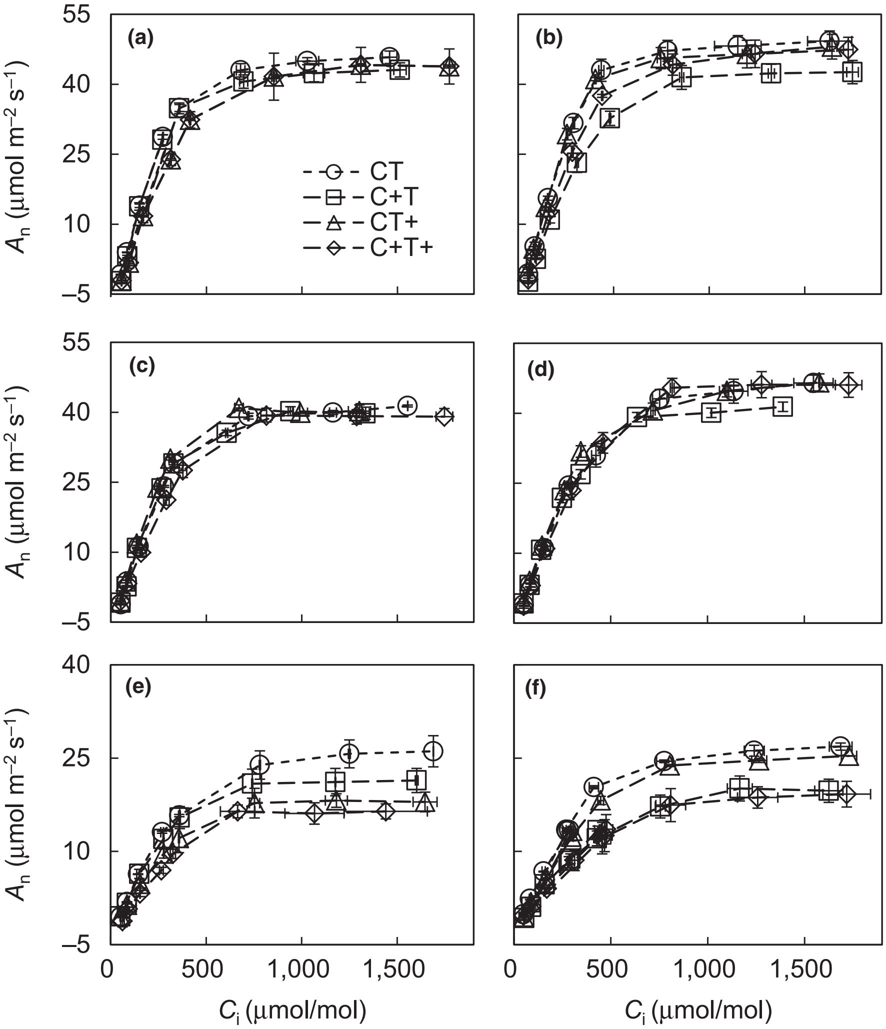

FIGURE 3 Examples of $A_n - C_i$ curves at I_{inc} of 2,000 μmol m^{-2} s^{-1} and leaf temperature of 33°C under ambient conditions (circles, CT), elevated CO_2 (squares, C+T), elevated temperature (triangles, CT+), and a combination of elevated CO_2 and elevated temperature (diamonds, C+T+) for cv. Changyou 5 (a, c, e) in the FACE 1 experiment and cv. Nanjing 9108 (b, d, f) in the FACE 2 experiment during the stem-elongating stage (a, b), heading stage (c, d), and grain-filling stage (e, f). Each data point represents the mean value of three replications (with bars for ± standard errors of the mean)

notably decreased A_n at high I_{inc} during the stem-elongating stage and grain-filling stage (Figure 2a,c and e), A_n at high C_i during the grain-filling stage (Figure 3a,c and e), and g_s at each I_{inc} during the stem-elongating stage and heading stage (Figure 4a,c and e), but notably increased g_s at each I_{inc} during the grain-filling stage. CT+ notably decreased A_n at each I_{inc} and C_i and g_s at high I_{inc} during the grain-filling stage, but notably increased g_s at low I_{inc} during the stem-elongating stage. C+T+ notably decreased A_n at high I_{inc} during the stem-elongating and heading stages, A_n at each I_{inc} and C_i during the grain-filling stage and g_s at high I_{inc} during the heading stage, but notably increased g_s at low I_{inc} during the stem-elongating stage and g_s at each I_{inc} during the grain-filling stage.

For Nanjing 9108 in the FACE 2 experiment, measurements at a leaf temperature of 33°C showed that compared with CT, C+T notably decreased A_n at high I_{inc} during the stem-elongating stage and A_n at each I_{inc} during the heading and grain-filling stages (Figure 2b,d and f), A_n at each C_i during the stem-elongating stage and grain-filling stage and A_n at high C_i during the heading stage (Figure 3b,d and f), and g_s at high I_{inc} during the stem-elongating stage and g_s at each I_{inc} during the heading stage and grain-filling stage (Figure 4b,d and f). CT+ notably decreased A_n at high I_{inc} during the stem-elongating stage and heading stages, A_n at each I_{inc} and C_i and g_s at each I_{inc} during the grain-filling stage, compared with CT. C+T+ notably decreased A_n at high I_{inc} during the stem-elongating stage and heading stages, A_n at low C_i during the stem-elongating stage, A_n at each I_{inc} and C_i and g_s at each I_{inc} during the grain-filling stage, compared with CT.

3.2 | Temperature response of light-saturated photosynthesis under four CO_2 and temperature treatments in FACE

For cv. Changyou 5 in the FACE 1 experiment, there were significant interaction effects between CO_2 and temperature on light-saturated photosynthesis ($A_{n,max}$) at 29°C during the stem-elongating stage (Figure 5a) and at 33°C during the heading stage (Figure 5c). Elevated CO_2 significantly decreased $A_{n,max}$ at all temperatures except at 29°C during the heading stage and at 33°C during the grain-filling stage (Figure 5a,c and e). Elevated temperature significantly decreased $A_{n,max}$ except $A_{n,max}$ at 36°C during the stem-elongating stage and at 39°C during the heading stage.

For cv. Nanjing 9108 in the FACE 2 experiment, interaction effects between CO_2 and temperature on $A_{n,max}$ were significant at 29°C during the stem-elongating stage and at 25, 29 and 39°C

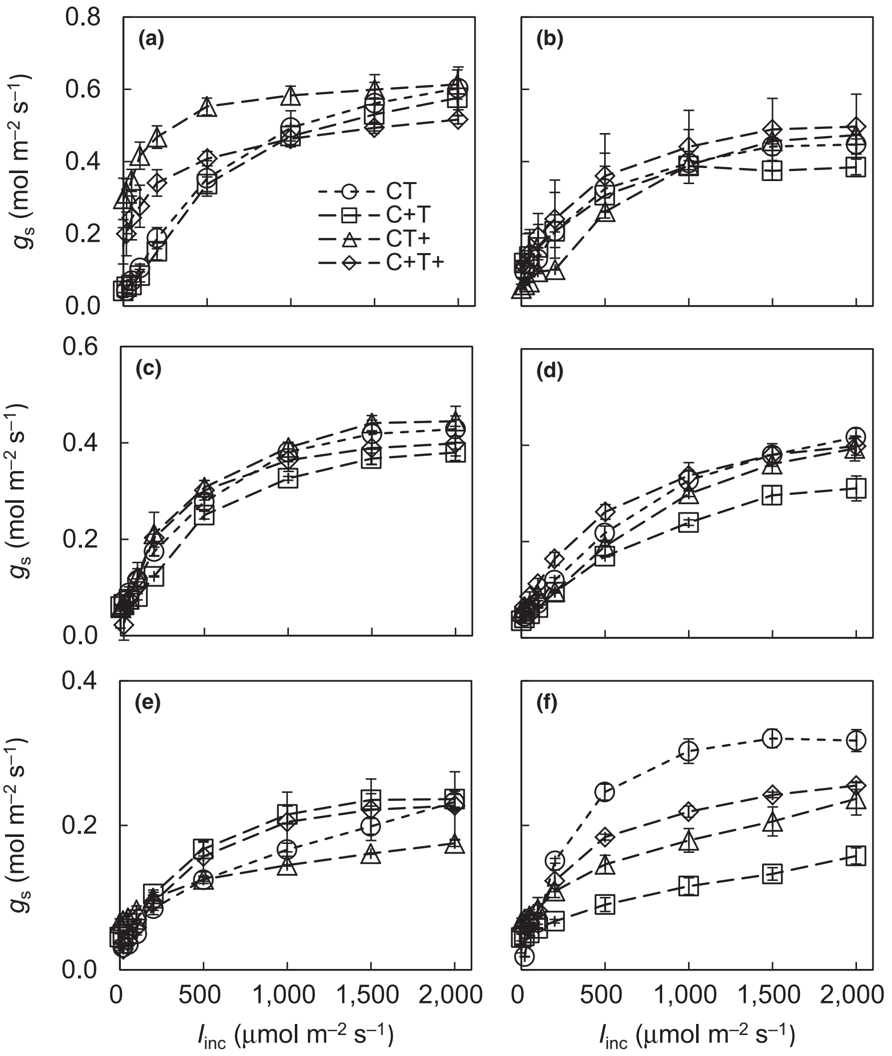

FIGURE 4 Examples of $g_s - I_{inc}$ curves at C_a of 380 μmol/mol and leaf temperature of 33°C under ambient conditions (circles, CT), elevated CO_2 (squares, C+T), elevated temperature (triangles, CT+), and a combination of elevated CO_2 and elevated temperature (diamonds, C+T+) for cv. Changyou 5 (a, c, e) in the FACE 1 experiment and cv. Nanjing 9108 (b, d, f) in the FACE 2 experiment during the stem-elongating stage (a, b), heading stage (c, d), and grain-filling stage (e, f). Each data point represents the mean value of three replications (with bars for ± standard errors of the mean)

during the heading stage (Figure 5b and d). Elevated CO_2 significantly decreased $A_{n,max}$ at all temperatures except at 39°C during the heading stage (Figure 5b,d and f). Elevated temperature significantly increased $A_{n,max}$ at 39°C during the stem-elongating stage and at 25°C during the heading stage, but significantly decreased $A_{n,max}$ at 39°C during the heading stage and at 36°C during the grain-filling stage.

3.3 | Model parameterization

As an example of the results, the responses of estimated R_d, J_{max}, V_{cmax}, and g_m to temperature for the CT treatment for the two rice cultivars grown in the two FACE systems are shown in Figure 6. All parameters were reliably estimated, as standard error values of the mean were relatively small (Tables 2–5).

3.4 | Estimated biochemical parameters in response to elevated CO_2 and temperature

For cv. Changyou 5 in the FACE 1 experiment, there were significant interaction effects between CO_2 and temperature on κ_{2LLmax} during the stem-elongating stage and on V_{cmax25} during the grain-filling stage (Table 2). Elevated CO_2 significantly increased R_{d25}, J_{max25}/V_{cmax25} and R_{d25}/V_{cmax25} before heading. Elevated temperature significantly increased E_{Jmax} and T_{opt} for J_{max} during the heading stage, but significantly decreased J_{max25}, κ_{2LLmax}, V_{cmax25} and J_{max25}/V_{cmax25} after heading.

For cv. Nanjing 9108 in the FACE 2 experiment, there were significant interaction effects between CO_2 and temperature on J_{max25}, κ_{2LLmax} and V_{cmax25} after heading (Table 3). Elevated CO_2 significantly increased R_{d25}/V_{cmax25} during the heading stage, but significantly decreased J_{max25} and κ_{2LLmax} after heading and V_{cmax25}. Elevated temperature significantly increased R_{d25}, J_{max25} and κ_{2LLmax} before heading.

3.5 | Estimated conductance parameters in response to elevated CO_2 and temperature

For cv. Changyou 5 in the FACE 1 experiment, there were significant interaction effects between CO_2 and temperature on g_{m25} during the grain-filling stage (Table 4). Elevated CO_2 significantly decreased g_{m25} during the stem-elongating and grain-filling stages and g_0 during

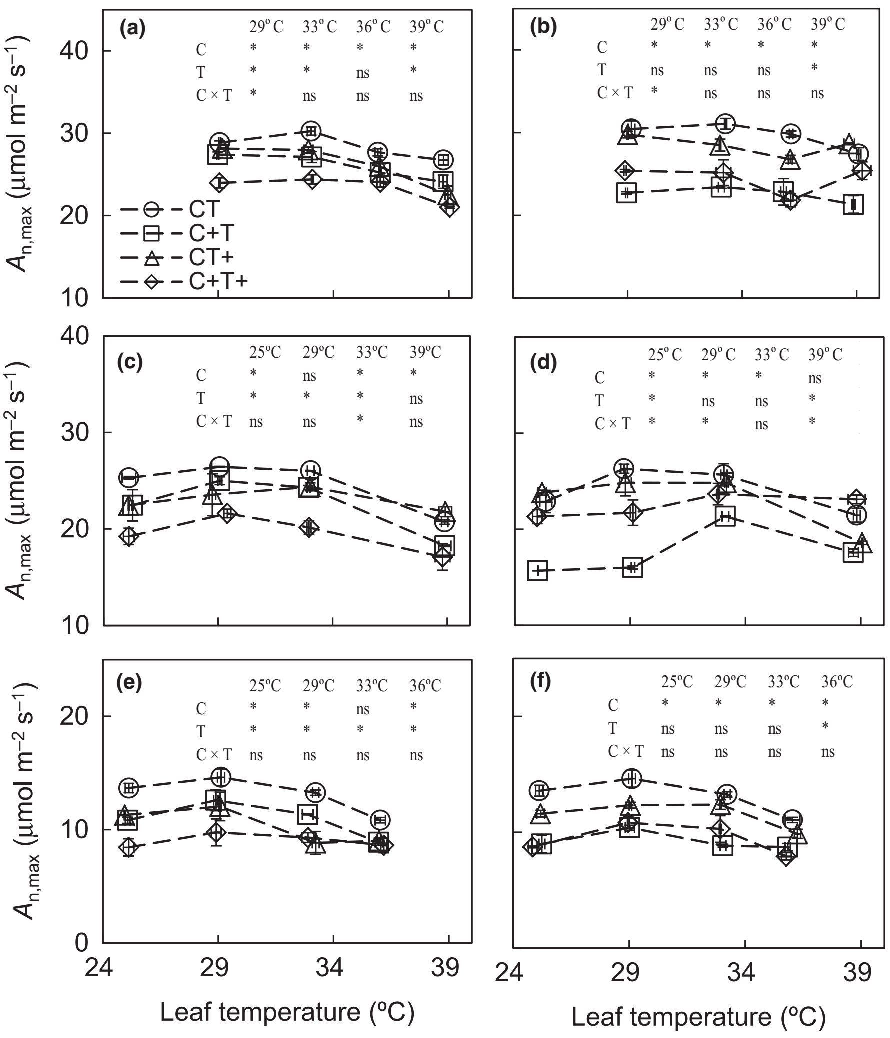

FIGURE 5 The temperature response of light-saturated photosynthesis ($A_{n,max}$) at I_{inc} of 2,000 μmol m^{-2} s^{-1} and C_a of 380 μmol/mol for cv. Changyou 5 (a, c, e) in the FACE 1 experiment and cv. Nanjing 9108 (b, d, f) in the FACE 2 experiment during the stem-elongating stage (a, b), heading stage (c, d), and grain-filling stage (e, f) under ambient condition (circles), elevated CO_2 (squares), elevated temperature (triangles), and the combination of elevated CO_2 and elevated temperature (diamonds). Each data point represents the mean value of three replications (with bars for ± standard errors of the mean). C and T stand for CO_2 and temperature, respectively, in FACE. Statistically significant differences ($p < .05$) and non-statistical significance are shown in the figure

the stem-elongating stage. Elevated temperature significantly increased g_0 before heading.

For cv. Nanjing 9108 in the FACE 2 experiment, there were no significant interaction effects between CO_2 and temperature on g_{m25}, E_{gm}, T_{opt} for g_m, a_1, b_1 and g_0 (Table 5). Elevated CO_2 significantly decreased g_{m25} during the grain-filling stage. Elevated temperature significantly increased g_0 after heading.

3.6 | The relationship between leaf nitrogen content and photosynthetic parameters

For cv. Changyou 5 in the FACE 1 experiment, R_{d25}, J_{max25}, V_{cmax25}, g_{m25} and κ_{2LLmax} increased with an increase in leaf nitrogen content (Figure 7). Values of N_b (see Equations 12–15) did not differ significantly among treatments, nor among parameters R_{d25}, J_{max25}, V_{cmax25}, and g_{m25}; so, a common N_b of 0.25 g N m^{-2} was estimated (Table 6). C+T significantly increased X_{Rd}, but significantly decreased X_{Vcmax} and X_{gm}, compared with CT (Table 6). CT+ significantly decreased X_{Vcmax}, compared with CT (Table 6). C+T+ significantly increased X_{Rd} and $X_{\kappa2LL}$, but significantly decreased X_{Vcmax} and X_{gm}, compared with CT (Table 6).

3.7 | Comparisons of model predictions between using acclimation photosynthesis parameters and non-acclimation photosynthesis parameters

The FvCB model parameterized for cv. Changyou 5 from the 2016 experiment not only described well A_n of this cultivar in 2016 but also predicted its A_n in 2014, with a similarly high coefficient of determination (r^2) and a low rRMSE between the two years (Figure 8). As expected, the model using treatment-specific parameters (i.e. assuming acclimation to growth CO_2 and temperature conditions) gave satisfactory estimations of A_n (Figure 8). The simulated A_n for C+T, CT+ and C+T+ using the CT-treatment parameters (including parameters X_{Rd}, X_{Jmax}, X_{Vcmax}, X_{gm25} and the linear relationship between κ_{2LLmax} and leaf nitrogen content), were almost equally satisfactory as predictions using parameter values of own treatments (Figure 8). Compared with the predictions using treatment-specific photosynthesis parameters, those using parameters of the CT treatment overestimated A_n for C+T by 4% and 7%, for CT+ by 1% and 1%, and for C+T+ by 3% and 5% for cv. Changyou 5 in 2014 and 2016, respectively. The little difference in both years between the two sets of prediction was surprising, given the

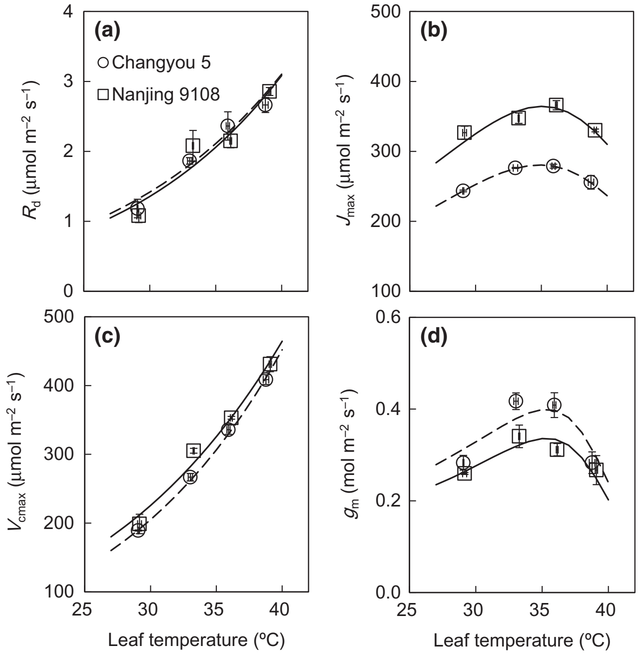

FIGURE 6 Examples of the temperature response of R_d (a), J_{max} (b), V_{cmax} (c), and g_m (d) under ambient conditions for cv. Changyou 5 (circles) in the FACE 1 experiment and cv. Nanjing 9108 (squares) in the FACE 2 experiment during the stem-elongating stage. Each data point represents the mean value of three replications (with bars for ± standard errors of the mean)

results we showed earlier (Tables 2, 3 and 6) that some parameters did acclimate to growth conditions concerning CO_2 and temperature.

Predictions of g_s by the BWB-Leuning-Yin model assuming acclimation to growth conditions also gave satisfactory estimations with a relatively high coefficient of determination and a low rRMSE under elevated CO_2 and elevated temperature for two rice cultivars in 2016 (Fig. S6). Compared with the predictions using acclimation photosynthesis parameters (Fig. S6), those using non-acclimation photosynthesis parameters, i.e. using the CT-treatment parameters (Fig. S7) underestimated g_s values for C+T by 3% and −1%, for CT+ by 25% and 12%, and for C+T+ by 19% and 10% for cv. Changyou 5 and cv. Nanjing 9108 in 2016, respectively. Meanwhile, r^2 values for the relationship between measured and simulated g_s using estimated a_1, b_1 and g_0 under CT for C+T, CT+ and C+T+ were generally decreased and rRMSE values were notably increased (Figs S6 and S7).

Despite the above significant impact on the prediction of g_s if no acclimation was assumed, it did not have a significant carry-over effect on the predictions of A_n as revealed by the analysis using the coupled FvCB and BWB-Leuning-Yin model in 2016 for Changyou 5 (Fig. S8a,c,e) and for Nanjing 9108 (Fig. S9). The same can be found when using the 2016 parameters for predicting A_n observed in the independent FACE experiment for Changyou 6 in 2014 (Figure 9a,c,e). Compared with simulations using treatment-specific g_s-parameters at each stage, simulations by the coupled model using the CT-treatment g_s parameters underestimated A_n only by 1%, 2% and 2% under C+T, CT+ and C+T+, respectively (Figure 9a,c,e).

Next we assessed the impact of assuming no acclimation of both FvCB and g_s parameters. Compared with simulations using treatment-specific FvCB and g_s parameters, simulations by the coupled FvCB and BWB-Leuning-Yin model using the CT-treatment FvCB and g_s parameters underestimated A_n only by −5%, 5% and 4% under C+T, CT+ and C+T+, respectively, of the 2016 experiment (Fig. S8b,d,f), and by 0%, 3% and 2% under the three treatments of the 2014 experiment (Figure 9b,d,f).

4 | DISCUSSION

4.1 | Needs to study the effects of both elevated CO_2 and temperature on photosynthesis and photosynthetic parameters

Climate change is strongly impacting crop productivity, and crop models have been used to quantitatively assess this impact. Of climate change variables, the impact of elevated atmospheric CO_2 has been most studied. Elevated CO_2 partly suppresses photorespiration and thus, at least, in a short-term, enhances leaf photosynthesis of C_3 species, which leads to enhanced growth and increased crop yields (Kim, Lieffering, Kobayashi, Okada, & Miura, 2003; Kimball, 1983; Sakai, Hasegawa, & Kobayashi, 2006). Most existing crop models that take this CO_2-enhancing effect into account, however, generally over-estimate the effect of elevated CO_2 on crop growth and yield under field conditions (Ainsworth, Leakey, Ort, & Long, 2008). Yin (2013) inferred that this overestimation could stem from the lack of mechanisms in the models that can predict the gradual decline of leaf N content of crops exposed to long-term elevated CO_2, relative to ambient conditions, with advancing crop growth, and this decline of leaf N partly reflects the acclimation of photosynthesis parameters to the whole-season elevated CO_2.

Climate change variables also involve increased temperature, and temperature is known to have a multiple effect on photosynthesis. For example, increasing temperature increases photorespiration, and therefore, may negate the effect of elevated CO_2 in suppressing photorespiration. Like that of elevated CO_2, the effect of temperature may differ between short- and long-terms. So, the impact of increased temperature should be quantified in combination with the effect of CO_2 under field conditions. In this study we measured leaf photosynthesis of rice plants grown at each of the factorial combinations of two levels of CO_2 and two levels of temperature under two FACE systems. The obtained light-, CO_2-and temperature-response curves of leaf photosynthesis (Figures 2, 3, 5 and S2–S4) were altered significantly by FACE CO_2 and temperature conditions. The associated stomatal conductance was even more strongly affected (Figure 4). In order to identify which parameters contributed to these effects and also in view of application to quantitative model assessment of the impact of climate change

TABLE 2 Parameter estimates (their standard errors in brackets) of the temperature response function for R_d, J_{max}, κ_{2LL}, and V_{cmax} under ambient CO_2 (CT), elevated CO_2 (C+T), elevated temperature (CT+) and the combination of elevated CO_2 and elevated temperature (C+T+) for stem-elongating, heading, and grain-filling stages of cv. Changyou 5 in the FACE 1 experiment in 2016

							Probability of significance		
	Parameter	Stage	CT	C+T	CT+	C+T+	C	T	C × T
R_d	R_{d25} (μmol m^{-2} s^{-1})	Elongating	0.94 (0.09)	1.25 (0.05)	1.06 (0.09)	1.33 (0.11)	*	ns	ns
		Heading	0.88 (0.04)	1.04 (0.17)	0.87 (0.14)	1.20 (0.08)	ns	ns	ns
		Grain-filling	0.55 (0.09)	0.71 (0.09)	0.67 (0.04)	0.67 (0.09)	ns	ns	ns
	E_{Rd} (J/mol)	Elongating	60,879 (5,995)	47,295 (4,372)	40,869 (4,662)	48,884 (2,714)	ns	ns	ns
		Heading	60,943 (3,235)	45,714 (9,983)	40,361 (10,295)	46,411 (4,318)	ns	ns	ns
		Grain-filling	86,374 (13,902)	73,410 (11,430)	76,917 (7,547)	73,000 (10,141)	ns	ns	ns
J_{max}	J_{max25} (μmol m^{-2} s^{-1})	Elongating	200.2 (4.6)	199.8 (10.8)	188.7 (9.3)	181.9 (12.3)	ns	ns	ns
		Heading	209.6 (0.3)	204.2 (4.6)	193.7 (9.3)	178.1 (3.9)	ns	*	ns
		Grain-filling	106.1 (1.4)	97.5 (3.6)	71.1 (4.8)	66.6 (2.6)	ns	*	ns
	E_{Jmax} (J/mol)	Elongating	42,769 (2,559)	41,927 (3,805)	48,335 (4,299)	46,858 (3,652)	ns	ns	ns
		Heading	20,039 (33)	25,647 (1,763)	30,908 (3,563)	30,658 (2,649)	ns	*	ns
		Grain-filling	11,680 (1,978)	14,893 (3,089)	19,123 (4,989)	19,463 (2,344)	ns	ns	ns
	D_{Jmax} (J/mol)		203,540[a]						
	$T_{opt,Jmax}$ (°C)	Elongating	34.9 (0.3)	34.8 (0.4)	35.5 (0.4)	35.4 (0.4)	ns	ns	ns
		Heading	31.5 (0.0)	32.6 (0.3)	33.4 (0.5)	33.3 (0.4)	ns	*	ns
		Grain-filling	29.2 (0.7)	30.1 (0.8)	31.0 (1.3)	31.3 (0.5)	ns	ns	ns
κ_{2LL}	κ_{2LLmax} (mol/mol)	Elongating	0.286 (0.001)	0.290 (0.001)	0.289 (0.003)	0.285 (0.002)	ns	ns	*
		Heading	0.282 (0.001)	0.281 (0.001)	0.285 (0.005)	0.281 (0.005)	ns	ns	ns
		Grain-filling	0.235 (0.001)	0.230 (0.002)	0.217 (0.003)	0.218 (0.001)	ns	*	ns
	$T_{opt,\kappa 2LL}$ (°C)	Elongating	34.7 (0.2)	34.6 (0.2)	34.9 (0.0)	35.1 (0.3)	ns	ns	ns
		Heading	29.8 (0.3)	30.5 (0.1)	31.3 (0.8)	31.1 (0.4)	ns	ns	ns
		Grain-filling	27.0 (0.2)	27.6 (0.2)	28.0 (0.4)	28.1 (0.3)	ns	ns	ns
	Ω (°C)		18[a]						
V_{cmax}	V_{cmax25} (μmol m^{-2} s^{-1})	Elongating	138.8 (3.2)	129.1 (2.5)	128.9 (5.4)	122.3 (5.4)	ns	ns	ns
		Heading	126.0 (1.1)	114.1 (3.4)	108.5 (13.4)	92.7 (1.0)	ns	*	ns
		Grain-filling	61.7 (2.2)	53.4 (2.5)	43.1 (2.4)	45.5 (1.4)	ns	*	*
	E_{Vcmax} (J/mol)	Elongating	60,974 (1,160)	55,947 (3,218)	53,611 (2,967)	56,632 (2,920)	ns	ns	ns
		Heading	58,842 (1,356)	61,170 (2,363)	60,055 (8,950)	60,137 (2,394)	ns	ns	ns
		Grain-filling	51,992 (486)	53,380 (4,415)	47,838 (4,209)	46,119 (2,862)	ns	ns	ns
Ratio	J_{max25}/V_{cmax25}	Elongating	1.45 (0.06)	1.55 (0.10)	1.46 (0.01)	1.49 (0.06)	*	ns	ns
		Heading	1.66 (0.01)	1.79 (0.04)	1.82 (0.17)	1.92 (0.05)	ns	ns	ns
		Grain-filling	1.72 (0.07)	1.83 (0.06)	1.65 (0.10)	1.47 (0.07)	ns	*	ns
	R_{d25}/V_{cmax25}	Elongating	0.007 (0.001)	0.010 (0.001)	0.008 (0.001)	0.011 (0.000)	*	ns	ns
		Heading	0.007 (0.000)	0.009 (0.001)	0.009 (0.002)	0.013 (0.001)	*	ns	ns
		Grain-filling	0.009 (0.002)	0.013 (0.001)	0.016 (0.001)	0.015 (0.002)	ns	ns	ns

C and T stand for CO_2 and temperature, respectively, in FACE. ANOVA *p*-values are indicated in the table (*$p < .05$; ns, not significant).

[a] Values of parameters were estimated from our data and did not vary with CO_2, temperature and stage.

variables, we applied the widely used FvCB leaf photosynthesis model and a stomatal conductance model to analyse these measurements. Such analyses enable to gain better insights into whether biochemical parameters in the FvCB model and CO_2-diffusion parameters related to mesophyll conductance g_m and stomatal conductance g_s acclimate to elevated CO_2 and temperature under FACE environments.

4.2 | Acclimation responses in photosynthetic biochemical parameters to elevated CO_2 and temperature

Most research focused on photosynthesis acclimation responses in the biochemical processes to elevated CO_2 and elevated temperature (Alonso et al., 2009; Borjigidai et al., 2006; Rosenthal, Ruiz-

TABLE 3 Parameter estimates (their standard errors in brackets) of the temperature response function for R_d, J_{max}, κ_{2LL} and V_{cmax} under ambient CO_2 (CT), elevated CO_2 (C+T), elevated temperature (CT+) and the combination of elevated CO_2 and elevated temperature (C+T+) for stem-elongating, heading, and grain-filling stages of cv. Nanjing 9108 in the FACE 2 experiment in 2016

							Probability of significance		
	Parameter	Stage	CT	C+T	CT+	C+T+	C	T	C × T
R_d	R_{d25} (μmol m^{-2} s^{-1})	Elongating	0.89 (0.12)	1.07 (0.07)	1.12 (0.23)	1.07 (0.15)	ns	ns	ns
		Heading	0.84 (0.10)	0.86 (0.09)	0.97 (0.05)	1.03 (0.13)	ns	*	ns
		Grain-filling	0.56 (0.07)	0.53 (0.09)	0.54 (0.01)	0.44 (0.07)	ns	ns	ns
	E_{Rd} (J/mol)	Elongating	64,567 (6,493)	58,480 (1,563)	52,321 (14,674)	47,574 (8,795)	ns	ns	ns
		Heading	74,796 (10,729)	57,357 (5,292)	54,862 (11,601)	61,299 (14,849)	ns	ns	ns
		Grain-filling	85,386 (6,178)	73,948 (13,969)	66,947 (5,139)	75,230 (20,332)	ns	ns	ns
J_{max}	J_{max25} (μmol m^{-2} s^{-1})	Elongating	262.1 (7.5)	231.6 (4.2)	259.8 (25.1)	238.8 (7.8)	ns	ns	ns
		Heading	246.6 (7.1)	195.7 (3.7)	248.7 (2.9)	227.3 (4.2)	*	*	*
		Grain-filling	105.0 (1.4)	74.5 (1.9)	99.7 (0.9)	79.0 (1.8)	*	ns	*
	E_{Jmax} (J/mol)	Elongating	42,394 (1,620)	44,806 (2,380)	44,152 (6,842)	46,409 (1,601)	ns	ns	ns
		Heading	24,825 (2,233)	27,223 (2,420)	28,488 (6,300)	31,391 (4,103)	ns	ns	ns
		Grain-filling	16,102 (3,080)	17,868 (5,866)	20,650 (3,223)	19,618 (1,841)	ns	ns	ns
	D_{Jmax} (J/mol)		203,540[a]						
	$T_{opt,Jmax}$ (°C)	Elongating	34.9 (0.2)	35.1 (0.3)	35.0 (0.8)	35.3 (0.2)	ns	ns	ns
		Heading	32.4 (0.4)	32.8 (0.4)	32.8 (1.1)	33.4 (0.6)	ns	ns	ns
		Grain-filling	30.5 (0.8)	30.5 (1.6)	31.6 (0.6)	31.4 (0.4)	ns	ns	ns
κ_{2LL}	κ_{2LLmax} (mol/mol)	Elongating	0.314 (0.001)	0.310 (0.001)	0.319 (0.000)	0.316 (0.002)	ns	*	ns
		Heading	0.278 (0.003)	0.275 (0.001)	0.285 (0.003)	0.281 (0.002)	ns	ns	ns
		Grain-filling	0.218 (0.002)	0.200 (0.001)	0.206 (0.003)	0.204 (0.002)	*	ns	*
	$T_{opt,\kappa 2LL}$ (°C)	Elongating	34.8 (0.7)	35.1 (0.1)	35.1 (0.2)	34.9 (0.3)	ns	ns	ns
		Heading	31.7 (0.0)	32.2 (0.0)	31.8 (0.2)	31.9 (0.4)	ns	ns	ns
		Grain-filling	28.4 (0.5)	28.6 (0.3)	29.0 (0.4)	29.0 (0.4)	ns	ns	ns
	Ω (°C)		18[a]						
V_{cmax}	V_{cmax25} (μmol m^{-2} s^{-1})	Elongating	155.6 (9.2)	115.7 (15.5)	145.9 (7.9)	116.1 (8.6)	*	ns	ns
		Heading	118.8 (1.5)	89.4 (4.2)	110.1 (4.4)	103.5 (4.7)	*	ns	*
		Grain-filling	60.5 (1.7)	40.4 (1.6)	53.0 (0.9)	46.3 (0.7)	*	ns	*
	E_{Vcmax} (J/mol)	Elongating	56,623 (4,194)	57,280 (9,126)	54,832 (2,463)	55,214 (5,851)	ns	ns	ns
		Heading	63,714 (1,263)	67,177 (2,932)	60,195 (5,115)	66,680 (4,740)	ns	ns	ns
		Grain-filling	46,438 (3,531)	50,103 (1,076)	52,143 (2,244)	49,490 (3,913)	ns	ns	ns
Ratio	J_{max25}/V_{cmax25}	Elongating	1.69 (0.05)	2.06 (0.22)	1.77 (0.09)	2.09 (0.20)	ns	ns	ns
		Heading	2.08 (0.06)	2.20 (0.12)	2.27 (0.11)	2.21 (0.14)	ns	ns	ns
		Grain-filling	1.74 (0.05)	1.85 (0.12)	1.88 (0.04)	1.71 (0.05)	ns	ns	ns
	R_{d25}/V_{cmax25}	Elongating	0.006 (0.001)	0.010 (0.002)	0.008 (0.001)	0.009 (0.001)	ns	ns	ns
		Heading	0.007 (0.001)	0.010 (0.001)	0.009 (0.001)	0.010 (0.001)	*	ns	ns
		Grain-filling	0.009 (0.001)	0.013 (0.003)	0.010 (0.000)	0.010 (0.001)	ns	ns	ns

C and T stand for CO_2 and temperature, respectively, in FACE. ANOVA *p*-values are indicated in the table (*$p < .05$; ns, not significant).
[a] Values of parameters were estimated from our data and did not vary with CO_2, temperature and stage.

Vera, Sievers, Bernacchi, & Ort, 2013). Some studies suggested that the down-regulation of photosynthesis under elevated CO_2 is caused by a decrease in J_{max} and V_{cmax} (Ainsworth & Long, 2005) and an increase in R_d (Alonso et al., 2009). Our results for cv. Nanjing 9108 in the FACE 2 experiment (Figures 2, 3, 5, S3 and S5, Table 3) confirmed these findings from literature, while the down-regulation of photosynthesis under elevated CO_2 for cv. Changyou 5 in the FACE 1 experiment was associated with a notable decrease in J_{max} during the grain-filling stage and V_{cmax} during all stages, and a notable increase in R_d (Figures 2, 3, 5, S2 and S4, Table 2). However, there were no consistent results for the effects of elevated temperature on photosynthesis (Adachi et al., 2014; Chi et al., 2013; Niu et al., 2008). Our results showed that elevated temperature significantly decreased both J_{max25} and V_{cmax25} after heading for cv. Changyou 5

TABLE 4 Parameter estimates (their standard errors in brackets) of the temperature response function for g_m, a_1, b_1 and g_0 under ambient CO_2 (CT), elevated CO_2 (C+T), elevated temperature (CT+) and the combination of elevated CO_2 and elevated temperature (C+T+) for stem-elongating, heading, and grain-filling stages of cv. Changyou 5 in the FACE 1 experiment in 2016, respectively

							Probability of significance		
	Parameter	Stage	CT	C+T	CT+	C+T+	C	T	C × T
g_m	g_{m25} (mol m^{-2} s^{-1})	Elongating	0.245 (0.025)	0.213 (0.011)	0.249 (0.028)	0.181 (0.006)	*	ns	ns
		Heading	0.218 (0.011)	0.184 (0.012)	0.200 (0.015)	0.176 (0.004)	ns	ns	ns
		Grain-filling	0.128 (0.013)	0.078 (0.009)	0.088 (0.001)	0.093 (0.010)	*	ns	*
	E_{gm} (J/mol)	Elongating	44,533 (6,970)	40,131 (6,406)	41,720 (10,648)	48,993 (3,447)	ns	ns	ns
		Heading	39,591 (5,307)	45,502 (12,243)	38,281 (7,231)	42,608 (10,069)	ns	ns	ns
		Grain-filling	37,787 (4,304)	33,569 (5,374)	35,506 (9,814)	44,636 (6,145)	ns	ns	ns
	$T_{opt,gm}$ (°C)	Elongating	35.4 (0.3)	35.2 (0.3)	35.2 (0.5)	35.6 (0.1)	ns	ns	ns
		Heading	35.2 (0.3)	35.3 (0.7)	35.1 (0.4)	35.3 (0.5)	ns	ns	ns
		Grain-filling	35.1 (0.2)	34.8 (0.3)	34.8 (0.7)	35.4 (0.3)	ns	ns	ns
g_s	a_1	Elongating	0.76 (0.04)	0.82 (0.07)	0.65 (0.11)	0.72 (0.03)	ns	ns	ns
		Heading	0.67 (0.03)	0.75 (0.03)	0.70 (0.01)	0.71 (0.01)	ns	ns	ns
		Grain-filling	0.75 (0.01)	0.73 (0.03)	0.80 (0.02)	0.76 (0.06)	ns	ns	ns
	b_1 (kPa^{-1})	Elongating	0.035 (0.026)	0.058 (0.034)	0.005 (0.047)	0.025 (0.027)	ns	ns	ns
		Heading	0.030 (0.019)	0.060 (0.014)	0.024 (0.008)	0.027 (0.008)	ns	ns	ns
		Grain-filling	0.046 (0.007)	0.032 (0.002)	0.049 (0.018)	0.018 (0.029)	ns	ns	ns
	g_0 (mol m^{-2} s^{-1})	Elongating	0.042 (0.008)	0.038 (0.003)	0.151 (0.012)	0.105 (0.019)	*	*	ns
		Heading	0.040 (0.005)	0.025 (0.006)	0.044 (0.001)	0.060 (0.008)	ns	*	ns
		Grain-filling	0.031 (0.001)	0.031 (0.000)	0.039 (0.003)	0.021 (0.007)	ns	ns	ns

C and T stand for CO_2 and temperature, respectively, in FACE. ANOVA p-values are indicated in the table (*$p < .05$; ns, not significant).

TABLE 5 Parameter estimates (their standard errors in brackets) of the temperature response function for g_m, a_1, b_1 and g_0 under ambient CO_2 (CT), elevated CO_2 (C+T), elevated temperature (CT+) and the combination of elevated CO_2 and elevated temperature (C+T+) for stem-elongating, heading, and grain-filling stages of cv. Nanjing 9108 in the FACE 2 experiment in 2016, respectively

							Probability of significance		
	Parameter	Stage	CT	C+T	CT+	C+T+	C	T	C × T
g_m	g_{m25} (mol m^{-2} s^{-1})	Elongating	0.204 (0.023)	0.159 (0.011)	0.182 (0.016)	0.157 (0.009)	ns	ns	ns
		Heading	0.205 (0.026)	0.146 (0.014)	0.174 (0.004)	0.162 (0.007)	ns	ns	ns
		Grain-filling	0.122 (0.021)	0.080 (0.006)	0.095 (0.004)	0.085 (0.010)	*	ns	ns
	E_{gm} (J/mol)	Elongating	46,164 (8,768)	46,356 (6,087)	46,589 (6,196)	38,992 (1,077)	ns	ns	ns
		Heading	46,685 (6,390)	4,4362 (10,891)	38,211 (6,968)	42,608 (6,310)	ns	ns	ns
		Grain-filling	42,618 (13,137)	38,590 (8,249)	33,786 (8,977)	42,616 (10,391)	ns	ns	ns
	$T_{opt,gm}$ (°C)	Elongating	35.5 (0.4)	35.5 (0.3)	35.5 (0.3)	35.2 (0.1)	ns	ns	ns
		Heading	35.5 (0.3)	35.3 (0.5)	35.1 (0.4)	35.6 (0.3)	ns	ns	ns
		Grain-filling	35.2 (0.6)	35.1 (0.5)	34.7 (0.6)	35.2 (0.5)	ns	ns	ns
g_s	a_1	Elongating	0.74 (0.03)	0.72 (0.00)	0.72 (0.02)	0.75 (0.01)	ns	ns	ns
		Heading	0.68 (0.05)	0.69 (0.07)	0.74 (0.05)	0.67 (0.06)	ns	ns	ns
		Grain-filling	0.83 (0.03)	0.82 (0.00)	0.84 (0.03)	0.86 (0.02)	ns	ns	ns
	b_1 (kPa^{-1})	Elongating	0.064 (0.017)	0.042 (0.008)	0.032 (0.008)	0.052 (0.010)	ns	ns	ns
		Heading	0.033 (0.028)	0.046 (0.032)	0.056 (0.022)	0.022 (0.029)	ns	ns	ns
		Grain-filling	0.074 (0.034)	0.056 (0.004)	0.064 (0.021)	0.078 (0.020)	ns	ns	ns
	g_0 (mol m^{-2} s^{-1})	Elongating	0.082 (0.006)	0.070 (0.011)	0.065 (0.019)	0.077 (0.004)	ns	ns	ns
		Heading	0.026 (0.002)	0.027 (0.003)	0.037 (0.001)	0.060 (0.008)	ns	*	ns
		Grain-filling	0.033 (0.003)	0.034 (0.000)	0.059 (0.008)	0.046 (0.004)	ns	*	ns

C and T stand for CO_2 and temperature, respectively, in FACE. ANOVA p-values are indicated in the table (*$p < .05$; ns, not significant).

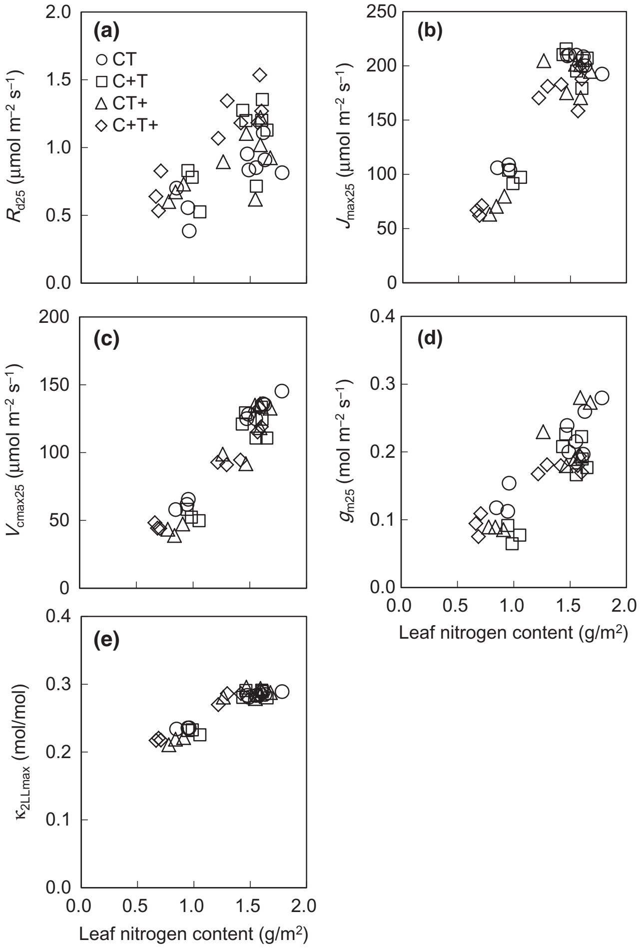

FIGURE 7 Relationships between R_{d25} (a), J_{max25} (b), V_{cmax25} (c), g_{m25} (d) or κ_{2LLmax} (e) and leaf nitrogen content for cv. Changyou 5 under four CO_2 and temperature combinations in the FACE 1 experiment

in the FACE 1 experiment (Table 2), while elevated temperature significantly increased J_{max25} before heading, but had no significant effects on V_{cmax25} for cv. Nanjing 9108 in the FACE 2 experiment (Table 3). Elevated temperature significantly decreased $A_{n,max}$ at 25°C after heading for cv. Changyou 5 in the FACE 1 experiment, but significantly increased $A_{n,max}$ at 25°C during the heading stage for cv. Nanjing 9108 in the FACE 2 experiment (Figure 5). This difference in photosynthesis response to elevated temperature may be related to higher mean daily air temperature during the whole cycle and warming magnitude for cv. Changyou 5 in the FACE 1 experiment than for cv. Nanjing 9108 in the FACE 2 experiment (Table 1). Liang, Xia, Liu, and Wan (2013) found that the enhancement of photosynthesis by elevated temperature decreased linearly with increasing growth temperature under ambient condition. In particular, our results showed that there were significant interaction effects between CO_2 and temperature on V_{cmax25} during the grain-filling stage for cv. Changyou 5 (Table 2) and on J_{max25}, V_{cmax25} and $A_{n,max}$ at 25°C after heading for cv. Nanjing 9108 (Figure 5d, Table 3).

Some studies fixed the J_{max}/V_{cmax} ratio and R_d/V_{cmax} ratio at 25°C at a constant value to parameterize the FvCB model (Borjigidai et al., 2006; Müller et al., 2005; von Caemmerer, 2000), an approach that was criticized by Archontoulis, Yin, Vos, Danalatos, and Struik (2011). Elevated CO_2 increased J_{max25}/V_{cmax25} (Ainsworth & Long, 2005), which was consistent with our results (Tables 2 and 3). Moreover, our results showed that elevated CO_2 significantly increased R_{d25}/V_{cmax25} before heading for both rice cultivars (Tables 2 and 3). Some studies found that J_{max}/V_{cmax} ratio at 25°C decreased with increasing growth temperature (Kattge & Knorr, 2007; Lin, Medlyn, De Kauwe, & Ellsworth, 2013). The increase in J_{max25}/V_{cmax25} ratio during crop development for cv. Changyou 5 (Table 2) may be related to the decrease in growth temperature during crop development (Fig. S1a). In addition, our results showed that elevated temperature significantly decreased J_{max25}/V_{cmax25} during the grain-filling stage for cv. Changyou 5 in 2016 (Table 2). Thus approaches that fix the J_{max25}/V_{cmax25} ratio and R_{d25}/V_{cmax25} at a constant value to parameterize the FvCB model should receive critical reservation for the effect of elevated CO_2 and elevated temperature.

The temperature dependence of carboxylation by Rubisco is stable among C_3 plants (Badger, Bjorkman, & Armond, 1982; Brooks & Farquhar, 1985). Our E_{Vcmax} estimates were indeed unaffected by elevated CO_2 and elevated temperature treatments (Tables 2 and 3), consistent with Alonso et al. (2009) and Chi et al. (2013). However, E_{Jmax} was significantly increased by elevated temperature for cv.

TABLE 6 Model estimates (*SE*) for photosynthetic parameters in relation to leaf N content, Equations (12–16), under ambient CO_2 (CT), elevated CO_2 (C+T), elevated temperature (CT+), and the combination of elevated CO_2 and elevated temperature (C+T+) for cv. Changyou 5 in the FACE 1 experiment in 2016[a]

		CT	C+T	CT+	C+T+
R_{d25}	X_{Rd} (μmol CO_2 g^{-1} N s^{-1})	0.69 (0.06)	0.89* (0.06)	0.79 (0.06)	1.08* (0.07)
J_{max25}	X_{Jmax} (μmol e$^-$ g^{-1} N s^{-1})	152.4 (6.2)	151.2 (6.3)	145.9 (6.5)	148.9 (7.1)
V_{cmax25}	X_{Vcmax} (μmol CO_2 g^{-1} N s^{-1})	97.9 (3.1)	90.1* (3.1)	91.5* (3.3)	90.8* (3.5)
g_{m25}	X_{gm} (mol g^{-1} N s^{-1})	0.18 (0.01)	0.15* (0.01)	0.17 (0.01)	0.15* (0.01)
κ_{2LLmax}	$X_{\kappa 2LL}$ (mol mol^{-1} m^2 g^{-1} N)	0.080 (0.002)	0.081 (0.002)	0.083 (0.002)	0.086* (0.002)
	k (mol/mol)	0.158[b] (0.006)	–	–	–

[a] The common N_b, 0.25(0.04) g N m^{-2}, for R_{d25}, J_{max25}, V_{cmax25} and g_{m25} were estimated for all treatments (see the text).

[b] The overall k for κ_{2LLmax} was estimated for all treatments and was not significantly different from the values for each treatment ($p > .05$).

*Significantly different from the value for the CT treatment ($p < .05$).

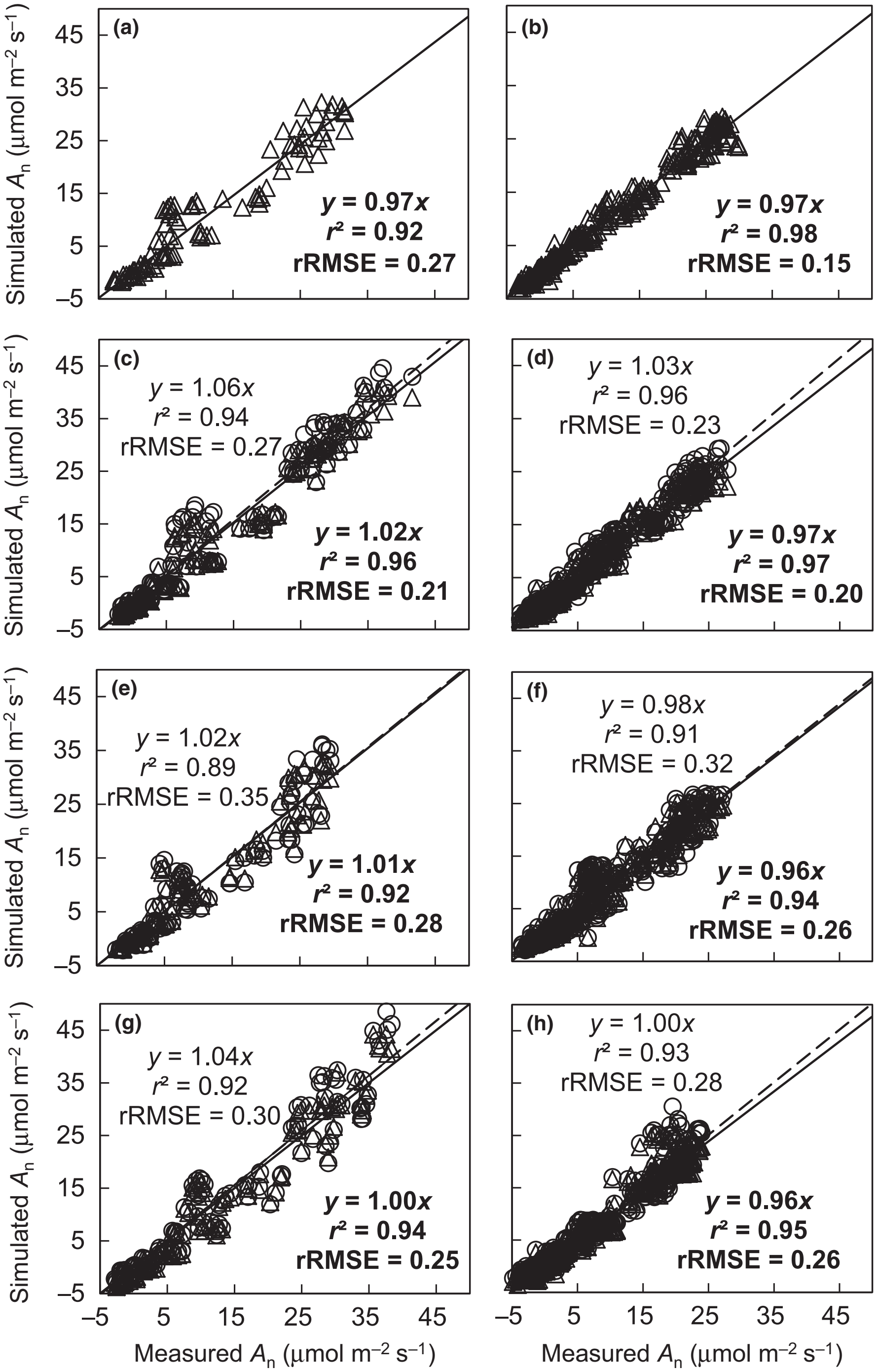

FIGURE 8 Comparisons of measured A_n of cv. Changyou 5 in the FACE 1 experiment in 2014 (a, c, e, g) and 2016 (b, d, f, h) with those simulated by the FvCB model (with C_i as input) either using treatment-specific photosynthesis parameters (triangles) or using the photosynthesis parameters derived only from the treatment under ambient conditions (circles), for the four FACE environments: ambient CO_2 and temperature (a, b), elevated CO_2 (c, d), elevated temperature (e, f), and a combination of elevated CO_2 and elevated temperature (g, h). Statistical parameters given in the panels are in bold (with full line) for predictions using treatment-specific parameter values and in non-bold (with dashed line) for predictions using parameter values derived from the ambient-condition treatment. The full or dashed line was fitted for all stages, when forcing the regression line through the origin

Changyou 5 during the heading stage (Table 2). Some studies found that the activation energy of J_{max} and V_{cmax} is positively related to plant growth temperature for single cases (Kattge & Knorr, 2007; Medlyn, Loustau, & Delzon, 2002; Onoda, Hikosaka, & Hirose, 2005). Our results showed that E_{Jmax}, E_{Vcmax} and T_{opt} for κ_{2LL} decreased during crop development, while E_{Rd} increased during crop development for both rice cultivars (Tables 2 and 3), which may be related to the decrease in growth temperature during crop development (Fig. S1a,b). κ_{2LL} was calculated by multiplying calibration factor s with Φ_{2LL} (see Equation 5), and the calibration factor s varied with temperature for cvs Changyou 5 and Nanjing 9108 (Table S1). The calibration factor s depends on absorptance by leaf photosynthetic pigments, proportion of absorbed photon flux density partitioned to photosystem II, and the fraction of alternative e^- transport pathways. Yin, van der Putten, Driever, and Struik (2016) suggested that the extent of any alternative e^- transport may depend on temperature. In addition, the temperature sensitivity of R_d was decreased by elevated CO_2 and elevated temperature (Alonso et al., 2009; Atkin et al., 2006; Chi et al., 2013; Crous et al., 2011), consistent with our results (Tables 2 and 3). The decrease in E_{Jmax} and E_{Vcmax} during crop development (Tables 2 and 3) resulted in a decrease in optimal temperature for $A_{n,max}$ during crop development

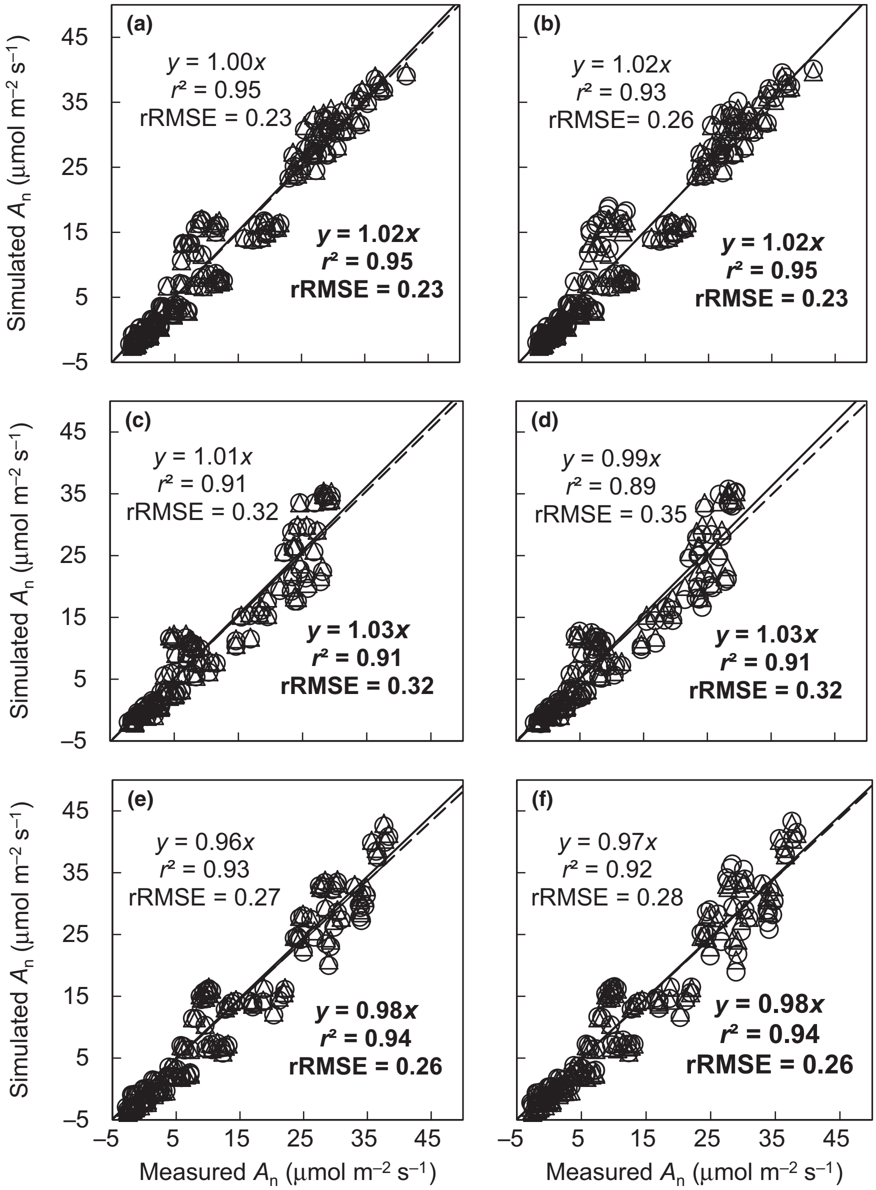

FIGURE 9 Comparisons of measured A_n of cv. Changyou 5 in the FACE 1 experiment in 2014 with those simulated by the coupled FvCB and BWB-Leuning-Yin model (with C_a as input) either using treatment-specific stomatal conductance parameters (triangles, a, c, e) or using the stomatal conductance parameters at each stage derived only from the treatment under ambient conditions (open circles, a, c, e), and either using treatment-specific FvCB and g_s parameters (triangles, b, d, f) or using the FvCB and g_s parameters at each stage derived only from the treatment under ambient conditions (open circles, b, d, f), for the three FACE environments: elevated CO_2 (a, b), elevated temperature (c, d), and a combination of elevated CO_2 and elevated temperature (e, f). Other details as in Figure 8

for cvs Changyou 5 and Nanjing 9108 (Figure 5). Our results showed that elevated temperature significantly decreased $A_{n,max}$ at 25, 29 and 33°C, but not at 39°C for cv. Changyou 5 during the heading stage in the FACE 1 experiment (Figure 5c). These temperature-response curves of $A_{n,max}$ were altered significantly by elevated temperature for cv. Changyou 5 during the heading stage in the FACE 1 experiment (Figure 5c), which may be related to the significant increase in E_{Jmax} under elevated temperature (Table 2).

Photosynthesis acclimation is frequently reported to be associated with a decrease in nitrogen concentration in the leaf and the entire plant (Drake et al., 1997; Stitt & Krapp, 1999). Photosynthesis is not strongly enhanced by long-term elevated CO_2 which may be associated with the inability of plants to acquire more nitrogen, resulting in lower leaf nitrogen content in plants grown under CO_2 enrichment (Drake et al., 1997; Luo et al., 2004; Peterson et al., 1999), which is consistent with our results for cv. Nanjing 9108 (Table S2). Elevated temperature significantly decreased leaf nitrogen content after heading for cv. Changyou 5, but significantly increased leaf nitrogen content at panicle initiation stage for cv. Nanjing 9108 (Table S2), which could be used to explain that elevated temperature significantly decreased both J_{max25} and V_{cmax25} after heading for cv. Changyou 5, but significantly increased J_{max25} before heading (Tables 2 and 3). Both J_{max25} and V_{cmax25} also showed high variation among rice genotypes and were linearly correlated with leaf nitrogen content (Gu, Yin, Stomph, Wang, & Struik, 2012). Higher J_{max25} and J_{max} in cv. Nanjing 9108 than in cv. Changyou 5 before heading (Figure 6, Tables 2 and 3) resulted in higher A_n at high C_i in cv. Nanjing 9108 than in cv. Changyou 5 (Figures 3, S4 and S5). J_{max25} and V_{cmax25} were much higher in cv. Nanjing 9108 than in cv. Changyou 5 before heading, which may be related to a higher SPAD value, an indicator of plant's nitrogen status on a leaf area basis (Peng, Laza, Garcia, & Cassman, 1995), in cv. Nanjing 9108 than in cv. Changyou 5 (Table S2). Yin (2013) found that elevated CO_2 did not change the relationships between J_{max25} or V_{cmax25} and leaf nitrogen content.

Our results showed that C+T changed the relationships between V_{cmax25} or R_{d25} and leaf nitrogen content, CT+ changed the relationships between V_{cmax25} and leaf nitrogen content, and C+T+ changed the relationships between V_{cmax25}, R_{d25} or κ_{2LLmax} and leaf nitrogen content for cv. Changyou 5 (Figure 7, Table 6). Elevated CO_2 decreased X_{Vcmax}, which was related to the decrease in the investment of leaf nitrogen in Rubisco under elevated CO_2 (Leakey et al., 2009; Sage, Sharkey, & Seemann, 1989). An increase in day respiration under elevated CO_2 may be because of the higher soluble carbohydrate content in the leaf (Alonso et al., 2009).

4.3 | Acclimation responses in diffusional conductances to elevated CO_2 and temperature

We used a peaked Arrhenius function to explore responses of mesophyll conductance g_m to temperature and the BWB-Leuning-Yin model to quantify stomatal conductance g_s in response to elevated CO_2 and elevated temperature. Our analysis showed that elevated CO_2 and elevated temperature caused strong acclimation of g_m and g_s for the two rice cultivars (Tables 4 and 5). These results were consistent with the finding that elevated CO_2 decreased g_m in rice (Zhu et al., 2012) and g_s showed strong acclimation to elevated CO_2 (Bunce, 2000, 2004) and elevated temperature (Pozo et al., 2005).

g_m acclimates and responds both in the long and short terms to many environmental variables, including temperature and CO_2, while the mechanistic basis of these acclimation responses remains unclear (Flexas et al., 2008). Our results showed that elevated CO_2 and elevated temperature significantly affected g_{m25}, but did not affect E_{gm} for the two rice cultivars (Tables 4 and 5). E_{gm} was kept relatively constant for different seasons (Zhu et al., 2011), which was consistent with our results (Tables 4 and 5). LMA is generally considered as setting a limitation for the maximum g_m (Flexas et al., 2008; Perez-Martin et al., 2009). Many studies showed that g_m decreased with increasing LMA (Flexas et al., 2008; Galmés et al., 2011; Gu et al., 2012). Our results showed that g_{m25} during the stem-elongating stage was higher for cv. Changyou 5 than for cv. Nanjing 9108 (Tables 4 and 5), a difference which may be related to a higher LMA value in cv. Nanjing 9108 than in cv. Changyou 5 (Table S2). Scafaro, von Caemmerer, Evans, and Atwell (2011) compared a cultivar of *Oryza sativa* with two wild *Oryza* relatives and found that the difference in mesophyll cell-wall thickness was responsible for variation in g_m. Zhu et al. (2012) found that cell wall thickness of rice did increase over time with elevated CO_2, consistent with the decline in g_m. However, the change of LMA results from the long-term environmental adaptation of the plants (Poorter, Niinemets, Poorter, Wright, & Villar, 2009), whereas g_m can vary quickly in response to environmental changes (Flexas et al., 2006). Many studies showed that leaf ageing strongly influenced g_m (Bernacchi, Morgan, Ort, & Long, 2005; Flexas et al., 2007) and there was a relatively strong linear correlation between g_m and leaf nitrogen content (von Caemmerer & Evans, 1991; Warren, 2004), consistent with our results (Tables 4 and 5, Figure 7d). The correlation between g_m and leaf nitrogen content may be explained by the surface area of the chloroplasts facing the cell walls, an anatomical determinant of g_m (Evans, von Caemmerer, Setchell, & Hudson, 1994; von Caemmerer & Evans, 1991), which depends on leaf nitrogen content.

The acclimation responses of stomatal conductance to elevated CO_2 and elevated temperature were reflected by the acclimation responses of the three parameters (a_1, b_1 and g_0). Many studies reported similar C_i/C_a ratios, close to 0.7, in both ambient and elevated growth CO_2 (Ainsworth, Rogers, Blum, Nösberger, & Long, 2003; Drake et al., 1997; Lodge, Dijkstra, Drake, & Morison, 2001). Our results showed that parameter a_1, approximately reflecting the C_i/C_a ratio for vapour saturated air (VPD approaches to zero), close to 0.7 for cv. Nanjing 9108 before heading and cv. Changyou 5, was unaffected by elevated CO_2 and elevated temperature (Tables 4 and 5). The value of a_1 was much higher than 0.7 during the grain-filling stage for cv. Nanjing 9108 (Table 5), which may have been caused by leaf senescence (Evans, 1986; Grossman-Clarke et al., 1999). Some studies showed g_s was sensitive (Yoshimoto, Oue, & Kobayashi, 2005) or less sensitive (Heath, 1998; Heath & Kerstiens, 1997) to VPD when grown at elevated CO_2 and less sensitive to VPD when grown at elevated temperature (Lewis, Lucash, Olszyk, & Tingey, 2002). Our results showed that $b_{1,}$ reflecting the sensitivity of g_s to VPD, was unaffected by elevated CO_2 and elevated temperature for both rice cultivars (Tables 4 and 5). However, the parameter g_0 was significantly decreased by elevated CO_2 for cv. Changyou 5 during the stem-elongating stage (Table 4), but significantly increased by elevated temperature for cv. Changyou 5 before heading (Figure 4a, Table 4) and for cv. Nanjing 9108 after heading (Table 5). In the literature, no consistent conclusions have been achieved on the effect of elevated CO_2 on g_0 (Bunce, 2000, 2004; Leakey, Bernacchi, et al., 2006; Leakey, Uribelarrea, et al., 2006; Medlyn et al., 2001). Many modelling studies fixed the value of g_0 at a constant value or at zero (De Kauwe et al., 2013). However, g_0 increased linearly with an increase in leaf nitrogen content (Zhang et al., 2017), which could be used to explain that g_0 decreased during crop development (Tables 4 and 5). Elevated temperature often increased g_0 (Tables 4 and 5), and physiological mechanisms for any effects of elevated CO_2 and temperature on g_0 merit further investigation.

4.4 | Do we need to consider the acclimation effect of photosynthesis parameters when projecting the effect of future climate change?

A coupled FvCB-stomatal conductance model, with incorporation of mesophyll conductance, is becoming a standard procedure in predicting leaf photosynthesis in response to climate change variables (e.g. Leakey, Bernacchi, et al., 2006; Leakey, Uribelarrea, et al., 2006; Li et al., 2012; Yin & Struik, 2009a). We, therefore, assessed, in three steps, whether taking into account the acclimation of model parameters yields a more accurate prediction of A_n under future climate change conditions: (1) considering the FvCB biochemical parameters, (2) considering g_s parameters, and (3) considering both FvCB and g_s parameters.

Our analysis of the first step showed that if the FvCB model incorporating nitrogen-based functional relationships between photosynthetic biochemical parameters and leaf nitrogen content (Figure 7, Table 6), did not take the acclimation responses of FvCB parameters into consideration, the simulated A_n was overestimated only by 3% and 5% for cv. Changyou 5 in 2014 and 2016, respectively, for the treatment with the combined elevated CO_2 and elevated temperature that best represents conditions of future global change (Figure 8).

Our analysis in the second step showed the importance of acclimation on the prediction of g_s per se: the simulations using the CT-treatment parameters at each stage overestimated values of g_s under C+T by −3% and 1%, and underestimated g_s under CT+ by 25% and 12% and under C+T+ by 19% and 10%, for cvs Changyou 5 and Nanjing 9108 in 2016, respectively (Figs S6 and S7). This indicated that g_s acclimated more to elevated temperature than to elevated CO_2. However, this impact of strong acclimation responses of g_s parameters became less important for predicting net photosynthesis rates A_n. The coupled FvCB and BWB-Leuning-Yin model using the CT-treatment g_s parameters at each stage underestimated A_n for C+T+ only by 2% in 2014 and by 3% in 2016 for cv. Changyou 5 (Figures 9e, S8f) and by 2% in 2016 for cv. Nanjing 9108 (Fig. S9c). This is because g_s directly influences C_i whereas C_i increases A_n only in a manner of diminishing return. The third step, indicated that the simulations by the coupled FvCB and BWB-Leuning-Yin model using the CT-treatment FvCB and g_s parameters at each stage underestimated A_n for C+T+ only by 2% in 2014 (Figure 9f) and by 4% in 2016 (Fig. S8f) for cv. Changyou 5. Therefore, a typical parameterization procedure that crop models using the FvCB and g_s models are estimated from data of plants grown under current ambient conditions will not result in critical errors when predicting leaf photosynthesis under conditions of elevated CO_2 and temperature of future climate.

Our measurements used Li-Cor to obtain g_s, whereas g_s measured at steady-states may not reflect real-time g_s at measurement times, as g_s is highly variable (Vialet-Chabrand, Dreyer, & Brendel, 2013). This implies that more sophisticated g_s models than the BWB-type models might be needed for more accurate prediction of stomatal behaviour. Furthermore, our experiments were conducted under conditions without water stress. Under climate change conditions where severe drought is expected, crop transpiration, which depends strongly on g_s, is a crucial variable to predict. Therefore, any acclimation responses of g_s parameters to elevated CO_2 and elevated temperature in combination with drought are essential for current crop models to accurately predict plant water use and crop microclimate under future global change (Shimono et al., 2010; Yoshimoto et al., 2005). How the FvCB parameters and parameters of more robust g_s models respond to elevated CO_2 and temperature in the presence of drought stress merits further quantification.

ACKNOWLEDGEMENTS

This research was funded by the Ministry of Agriculture of the Peoples' Republic of China (200903003), the National Natural Science Foundation of China (31261140364) and (31400372), State Administration of Foreign Experts Affairs of the People's Republic of China and Ministry of Education of the People's Republic of China (the 111 project, B16026) and was conducted in the framework of collaboration between the College of Agriculture, Nanjing Agricultural University and the Centre for Crop Systems Analysis, Wageningen University. The senior author thanks the China Scholarship Council and the Netherlands Organisation for International Cooperation in Higher Education (Nuffic) for awarding him a joint Sino-Dutch fellowship to conduct this work. PCS and XY contributed to the work via the ModCarboStress project of the ERA-NET Plus on Climate Smart Agriculture, funded by the Netherlands Organisation for Scientific Research (NWO). Many thanks go to Dr Xuhui Zhang and Dr Xiaoyu Liu of the College of Resources and Environmental Sciences, Nanjing Agricultural University, and Dr Gang Liu of State Key Laboratory of Soil and Sustainable Agriculture, Institute of Soil Science, Chinese Academy of Sciences for their technical supports during the FACE experimentation, Weilu Wang and Manman Yuan of State Key Laboratory of Soil and Sustainable Agriculture, Institute of Soil Science, Chinese Academy of Sciences for sharing data of leaf nitrogen concentration and leaf mass per area in cv. Nanjing 9108 in Table S2.

ORCID

Weihong Luo http://orcid.org/0000-0002-4505-3339
Xinyou Yin http://orcid.org/0000-0001-8273-8022

REFERENCES

Adachi, M., Hasegawa, T., Fukayama, H., Tokida, T., Sakai, H., Matsunami, T., . . . Okada, M. (2014). Soil and water warming accelerates phenology and down-regulation of leaf photosynthesis of rice plants grown under free-air CO_2 enrichment. *Plant Cell Physiology*, *55*, 370–380. https://doi.org/10.1093/pcp/pcu005

Ainsworth, E. A., Leakey, A. D. B., Ort, D. R., & Long, S. P. (2008). FACE-ing the facts: Inconsistencies and interdependence among field, chamber and modelling [CO_2] impacts on crop yield and food supply. *New Phytologist*, *179*, 5–9. https://doi.org/10.1111/nph.2008.179.issue-1

Ainsworth, E. A., & Long, S. P. (2005). What have we learned from 15 years of free-air CO_2 enrichment (FACE)? A meta-analytic review of the responses of photosynthesis, canopy properties and plant production to rising CO_2. *New Phytologist*, *165*, 351–372.

Ainsworth, E. A., Rogers, A., Blum, H., Nösberger, J., & Long, S. P. (2003). Variation in acclimation of photosynthesis in *Trifolium repens* after eight years of exposure to Free Air CO_2 Enrichment (FACE). *Journal of Experimental Botany*, *54*, 2769–2774. https://doi.org/10.1093/jxb/erg309

Alonso, A., Pérez, P., & Martínez-Carrasco, R. (2009). Growth in elevated CO_2 enhances temperature response of photosynthesis in wheat. *Physiologia Plantarum*, *135*, 109–120. https://doi.org/10.1111/ppl.2009.135.issue-2

Archontoulis, S. V., Yin, X., Vos, J., Danalatos, N. G., & Struik, P. C. (2011). Leaf photosynthesis and respiration of three bioenergy crops in relation to temperature and leaf nitrogen: How conserved are biochemical model parameters among crop species? *Journal of Experimental Botany*, *63*, 895–911.

Asseng, S., Jamieson, P. D., Kimball, B., Pinter, P., Sayre, K., Bowden, J. W., & Howden, S. M. (2004). Simulated wheat growth affected by rising temperature, increased water deficit and elevated atmospheric CO_2. *Field Crops Research*, *85*, 85–102. https://doi.org/10.1016/S0378-4290(03)00154-0

Atkin, O. K., Scheurwater, I., & Pons, T. L. (2006). High thermal acclimation potential of both photosynthesis and respiration in two lowland Plantago species in contrast to an alpine congeneric. *Global Change Biology*, *12*, 500–515. https://doi.org/10.1111/gcb.2006.12.issue-3

Badger, M. R., Bjorkman, O., & Armond, P. A. (1982). An analysis of photosynthetic response and adaptation to temperature in higher-plants – Temperature-acclimation in the desert evergreen *Nerium oleander* L. *Plant, Cell and Environment*, *5*, 85–99.

Ball, J. T., Woodrow, I. E., & Berry, J. A. (1987). A model predicting stomatal conductance and its contribution to the control of photosynthesis under different environmental conditions. In J. Biggens (Ed.), *Progress in photosynthesis research* (Vol. IV, pp. 221–224). Dordrecht, The Netherlands: Martinus-Nijhoff Publishers. https://doi.org/10.1007/978-94-017-0519-6

Bernacchi, C. J., Leakey, A. D. B., Heady, L. E., Morgan, P. B., Dohleman, F. G., Mcgrath, J. M., … Ort, D. R. (2006). Hourly and seasonal variation in photosynthesis and stomatal conductance of soybean grown at future CO_2 and ozone concentrations for 3 years under fully open-air field conditions. *Plant, Cell and Environment*, *29*, 2007–2090.

Bernacchi, C. J., Morgan, P. B., Ort, D. R., & Long, S. P. (2005). The growth of soybean under free air [CO_2] enrichment (FACE) stimulates photosynthesis while decreasing in vivo Rubisco capacity. *Planta*, *220*, 434–446. https://doi.org/10.1007/s00425-004-1320-8

Bernacchi, C. J., Portis, A. R., Nakano, H., von Caemmerer, S., & Long, S. P. (2002). Temperature response of mesophyll conductance; implications for the determination of Rubisco enzyme kinetics and for limitations to photosynthesis in vivo. *Plant Physiology*, *130*, 1992–1998. https://doi.org/10.1104/pp.008250

Bernacchi, C. J., Singsaas, E. L., Pimentel, C., Portis, A. R., & Long, S. P. (2001). Improved temperature response functions for models of Rubisco-limited photosynthesis. *Plant, Cell and Environment*, *24*, 253–259. https://doi.org/10.1111/pce.2001.24.issue-2

Borjigidai, A., Hikosaka, K., Hirose, T., Hasegawa, T., Okada, M., & Kobayashi, K. (2006). Seasonal changes in temperature dependence of photosynthetic rate in rice under a free-air CO_2 enrichment. *Annals of Botany*, *97*, 549–557. https://doi.org/10.1093/aob/mcl001

Braune, H., Müller, J., & Diepenbrock, W. (2009). Integrating effects of leaf nitrogen, age, and growth temperature into the photosynthesis-stomatal conductance model LEAFC3-N parameterized for barley (*Hordeum vulgare* L.). *Ecological Modelling*, *220*, 1599–1612. https://doi.org/10.1016/j.ecolmodel.2009.03.027

Brooks, A., & Farquhar, G. D. (1985). Effect of temperature on the CO_2/O_2 specificity of ribulose-1,5-bisphosphate carboxylase oxygenase and the rate of respiration in the light-estimates from gas-exchange measurements on spinach. *Planta*, *165*, 397–406. https://doi.org/10.1007/BF00392238

Bunce, J. A. (2000). Responses of stomatal conductance to light, humidity and temperature in winter wheat and barley grown at three concentrations of carbon dioxide in the field. *Global Change Biology*, *6*, 371–382. https://doi.org/10.1046/j.1365-2486.2000.00314.x

Bunce, J. A. (2004). Carbon dioxide effects on stomatal responses to the environment and water use by crops under field conditions. *Oecologia*, *140*, 1–10. https://doi.org/10.1007/s00442-003-1401-6

Cai, C., Yin, X., He, S., Jiang, W., Si, C., Struik, P. C., … Pan, G. (2016). Responses of wheat and rice to factorial combinations of ambient and elevated CO_2 and temperature in FACE experiments. *Global Change Biology*, *22*, 856–874. https://doi.org/10.1111/gcb.13065

Chi, Y., Xu, M., Shen, R., Yang, Q., Huang, B., & Wan, S. (2013). Acclimation of foliar respiration and photosynthesis in response to experimental warming in a temperate steppe in northern China. *PLoS ONE*, *8*, e56482. https://doi.org/10.1371/journal.pone.0056482

Crous, K. Y., Zaragoza-Castells, J., Löw, M., Ellsworth, D. S., Tissue, D. T., Tjoelker, M. G., … Atkin, O. K. (2011). Seasonal acclimation of leaf respiration in *Eucalyptus saligna* tree: Impacts of elevated atmospheric CO_2 conditions and summer drought. *Global Change Biology*, *17*, 1560–1576. https://doi.org/10.1111/gcb.2011.17.issue-4

De Kauwe, M. G., Medlyn, B. E., Zaehle, S., Walker, A. P., Dietze, M. C., Hickler, T., … Norby, R. J. (2013). Forest water use and water use efficiency at elevated CO_2: A model-data intercomparison at two contrasting temperate forest FACE sites. *Global Change Biology*, *19*, 1759–1779. https://doi.org/10.1111/gcb.12164

Dillaway, D. N., & Kruger, E. L. (2010). Thermal acclimation of photosynthesis: A comparison of boreal and temperate tree species along a latitudinal transect. *Plant, Cell and Environment*, *33*, 888–899. https://doi.org/10.1111/pce.2010.33.issue-6

Drake, B. G., González-Meler, M. A., & Long, S. P. (1997). More efficient plants: A consequence of rising atmospheric CO_2? *Annual Review of Plant Physiology and Plant Molecular Biology*, *48*, 609–639. https://doi.org/10.1146/annurev.arplant.48.1.609

Dreyer, E., Le Roux, X., Montpied, P., Daudet, A. F., & Masson, F. (2001). Temperature response of leaf photosynthetic capacity in seedlings from seven temperate tree species. *Tree Physiology*, *21*, 223–232. https://doi.org/10.1093/treephys/21.4.223

Evans, J. R. (1986). A comparison of the photosynthetic properties of flag leaves from *Triticum aestivum* and *T. monococcum*. In E. Jeffcoat & A. F. Stead (Eds.), *Regulation of sources and sinks in crop plants* (pp. 111–125). York, UK: British Plant Growth Regulator Group, Monograph No. 12.

Evans, J. R., von Caemmerer, S., Setchell, B., & Hudson, G. (1994). Transfer conductance and leaf anatomy in transgenic tobacco with a reduced content of Rubisco. *Australian Journal of Plant Physiology*, *21*, 475. https://doi.org/10.1071/PP9940475

Farquhar, G. D., von Caemmerer, S., & Berry, J. A. (1980). A biochemical model of photosynthetic CO_2 assimilation in leaves of C_3 species. *Planta*, *149*, 78–90. https://doi.org/10.1007/BF00386231

Flexas, J., Barbour, M. M., Brendel, O., Cabrera, H. M., Carriquí, M., Díaz-Espejo, A., … Warren, C. R. (2012). Mesophyll diffusion conductance to CO_2: An unappreciated central player in photosynthesis. *Plant Science*, *193–194*, 70–84. https://doi.org/10.1016/j.plantsci.2012.05.009

Flexas, J., Carriquí, M., Coopman, R. E., Gago, J., Galmés, J., Martorell, S., … Diaz-Espejo, A. (2014). Stomatal and mesophyll conductances to CO_2 in different plant groups: Underrated factors for predicting leaf photosynthesis responses to climate change? *Plant Science*, *226*, 41–48. https://doi.org/10.1016/j.plantsci.2014.06.011

Flexas, J., Ortuño, M. F., Ribas-Carbó, M., Diaz-Espejo, A., Florez-Sarasa, I. D., & Medrano, H. (2007). Mesophyll conductance to CO_2 in *Arabidopsis thaliana*. *New Physiologist*, *175*, 501–511. https://doi.org/10.1111/nph.2007.175.issue-3

Flexas, J., Ribas-Carbó, M., Bota, J., Galmés, J., Henkle, M., Martínez-Cañellas, S., & Medrano, H. (2006). Decreased Rubisco activity during water stress is not induced by decreased relative water content but related to conditions of low stomatal conductance and chloroplast CO_2 concentration. *New Phytologist*, *172*, 73–82. https://doi.org/10.1111/nph.2006.172.issue-1

Flexas, J., Ribas-Carbó, M., Diaz-Espejo, A., Galmés, J., & Medrano, H. (2008). Mesophyll conductance to CO_2: Current knowledge and future prospects. *Plant, Cell and Environment*, *31*, 602–621. https://doi.org/10.1111/j.1365-3040.2007.01757.x

Galmés, J., Conesa, M. À. M., Ochogavía, J. M., Perdomo, J. A., Francis, D. M., Ribas-Carbó, M., … Cifre, J. (2011). Physiological and morphological adaptations in relation to water use efficiency in Mediterranean accessions of *Solanum lycopersicum*. *Plant, Cell and Environment*, *34*, 245–260. https://doi.org/10.1111/pce.2011.34.issue-2

Genty, B., Briantais, J. M., & Baker, N. R. (1989). The relationship between the quantum yield of photosynthetic electron transport and quenching of chlorophyll fluorescence. *Biochimica et Biophysica Acta*, *990*, 87–92. https://doi.org/10.1016/S0304-4165(89)80016-9

Grossman-Clarke, S., Kimball, B. A., Hunsaker, D. J., Long, S. P., Garcia, R. L., Kartschall, T., … LaMorte, R. L. (1999). Effects of elevated atmospheric CO_2 on canopy transpiration in senescent spring wheat. *Agricultural and Forest Meteorology*, *93*, 95–109. https://doi.org/10.1016/S0168-1923(98)00111-7

Gu, J., Yin, X., Stomph, T. J., Wang, H., & Struik, P. C. (2012). Physiological basis of genetic variation in leaf photosynthesis among rice (*Oryza sativa* L.) introgression lines under drought and well-watered conditions. *Journal of Experimental Botany*, *63*, 5137–5153. https://doi.org/10.1093/jxb/ers170

Han, Y., Liu, G., Zhu, J. G., Okada, M., & Yoshimoto, M. (2002). Rice-wheat rotational FACE platform. II. Data processing software package (in Chinese). *Chinese Journal of Applied Ecology*, *13*, 1259–1263.

Harley, P. C., Thomas, R. B., Reynolds, J. F., & Strain, B. R. (1992). Modelling photosynthesis of cotton grown in elevated CO_2. *Plant, Cell and Environment*, *15*, 271–282. https://doi.org/10.1111/pce.1992.15.issue-3

Heath, J. (1998). Stomata of trees growing in CO_2-enriched air show reduce sensitivity to vapour pressure deficit and drought. *Plant, Cell and Environment*, *16*, 369–388.

Heath, J., & Kerstiens, G. (1997). Effects of elevated CO_2 on leaf gas exchange in beech and oak at two levels of nutrient supply: Consequences for sensitivity to drought in beech. *Plant, Cell and Environment*, *20*, 57–67. https://doi.org/10.1046/j.1365-3040.1997.d01-13.x

Hirose, T., Ackerly, D. D., Traw, M. B., Ramseirer, D., & Bazz, F. A. (1997). CO_2 elevation, canopy photosynthesis and optimal leaf area index. *Ecology*, *78*, 2339–2350.

Jing, L., Lai, S., Wang, Y., Yang, L., & Wang, Y. (2016). Combined effect of increasing atmospheric CO_2 concentration and temperature on growth and development of rice: A research review (in Chinese). *Acta Ecologica Sinica*, *36*, 4254–4265.

Jing, L., Wang, J., Shen, S., Wang, Y., Zhu, J., Wang, Y., & Yang, L. (2016). The impact of elevated CO_2 and temperature on grain quality of rice grown under open-air field conditions. *Journal of the Science of Food and Agriculture*, *96*, 3658–3667. https://doi.org/10.1002/jsfa.2016.96.issue-11

June, T., Evans, J. R., & Farquhar, G. D. (2004). A simple new equation for the reversible temperature dependence of photosynthetic electron transport: A study on soybean leaf. *Functional Plant Biology*, *31*, 275–283. https://doi.org/10.1071/FP03250

Kattge, J., & Knorr, W. (2007). Temperature acclimation in a biochemical model of photosynthesis: A reanalysis of data from 36 species. *Plant, Cell and Environment*, *30*, 1176–1190. https://doi.org/10.1111/pce.2007.30.issue-9

Kim, H. Y., Ko, J., Kang, S., & Tenhunen, J. (2013). Impacts of climate change on paddy rice yield in a temperature climate. *Global Change Biology*, *19*, 548–562. https://doi.org/10.1111/gcb.2012.19.issue-2

Kim, H. Y., Lieffering, M., Kobayashi, K., Okada, M., & Miura, S. (2003). Seasonal changes in the effects of elevated CO_2 on rice at three levels of nitrogen supply: A free air CO_2 enrichment (FACE) experiment. *Global Change Biology*, *9*, 826–837. https://doi.org/10.1046/j.1365-2486.2003.00641.x

Kimball, B. A. (1983). Carbon dioxide and agricultural yield: An assemblage and analysis of 430 prior observations. *Agronomy Journal*, *75*, 779–788. https://doi.org/10.2134/agronj1983.00021962007500050014x

Kimball, B. A., Conley, M. M., Wang, S., Lin, X. W., Luo, C. Y., Morgan, J., & Smith, D. (2008). Infrared heater arrays for warming ecosystem field plots. *Global Change Biology*, *14*, 309–320.

Kosugi, Y., Shibata, S., & Kobashi, S. (2003). Parameterization of the CO_2 and H_2O gas exchange of several temperate deciduous broad-leaved trees at the leaf scale considering seasonal changes. *Plant, Cell and Environment*, *26*, 285–301. https://doi.org/10.1046/j.1365-3040.2003.00960.x

Leakey, A. D. B., Ainsworth, E. A., Bernacchi, C. J., Rogers, A., Long, S. P., & Ort, D. R. (2009). Elevated CO_2 effects on plant carbon, nitrogen, and water relations: Six important lessons from FACE. *Journal of Experimental Botany*, *60*, 2859–2876. https://doi.org/10.1093/jxb/erp096

Leakey, A. D. B., Bernacchi, C. J., Ort, D. R., & Long, S. P. (2006). Long-term growth of soybean at elevated CO_2 does not cause acclimation of stomatal conductance under fully open-air conditions. *Plant, Cell and Environment*, *29*, 1794–1800. https://doi.org/10.1111/pce.2006.29.issue-9

Leakey, A. D. B., Uribelarrea, M., Ainsworth, E. A., Naidu, S. L., Rogers, A., Ort, D. R., & Long, S. P. (2006). Photosynthesis, productivity, and yield of maize are not affected by open-air elevation of CO_2 concentration in the absence of drought. *Plant Physiology*, *140*, 779–790. https://doi.org/10.1104/pp.105.073957

Leuning, R. (1995). A critical appraisal of a combined stomatal-photosynthesis model for C_3 plants. *Plant, Cell and Environment*, *18*, 339–355. https://doi.org/10.1111/pce.1995.18.issue-4

Lewis, J. D., Lucash, M., Olszyk, D. M., & Tingey, D. T. (2002). Stomatal responses of Douglas-fir seedlings to elevated carbon dioxide and temperature during the third and fourth years of exposure. *Plant, Cell and Environment*, *25*, 1411–1421. https://doi.org/10.1046/j.1365-3040.2002.00923.x

Li, T., Hasegawa, T., Yin, X., Zhu, Y., Boote, K., Adam, M., … Bouman, B. (2014). Uncertainties in predicting rice yield by current crop models under a wider a wide range of climatic conditions. *Global Change Biology*, *21*, 1328–1341.

Li, G., Lin, L., Dong, Y., An, D., Li, Y., Luo, W., … Zhao, C. (2012). Testing two models for the estimation of leaf stomatal conductance in four greenhouse crops cucumber, chrysanthemum, tulip and lilium. *Agricultural and Forest Meteorology*, *165*, 92–103. https://doi.org/10.1016/j.agrformet.2012.06.004

Liang, J., Xia, J., Liu, L., & Wan, S. (2013). Global patterns of the responses of leaf-level photosynthesis and respiration in terrestrial plants to experimental warming. *Journal of Plant Ecology*, *6*, 437–447. https://doi.org/10.1093/jpe/rtt003

Lin, Y. S., Medlyn, B. E., De Kauwe, M. G., & Ellsworth, D. S. (2013). Biochemical photosynthetic responses to temperature: How do interspecific differences compare with seasonal shifts? *Tree Physiology*, *33*, 793–806. https://doi.org/10.1093/treephys/tpt047

Liu, G., Han, Y., Zhu, J. G., Okada, M., Nakamura, H., & Yoshimoto, M. (2002). Rice-wheat rotational FACE platform. I. System construct and control (in Chinese). *Chinese Journal of Applied Ecology*, *13*, 1253–1258.

Lodge, R. J., Dijkstra, P. D., Drake, B. G., & Morison, J. I. L. (2001). Stomatal acclimation to increased CO_2 concentration in a Florida scrub oak species *Quercus myrtifolia* Willd. *Plant, Cell and Environment*, *24*, 77–88. https://doi.org/10.1046/j.1365-3040.2001.00659.x

Long, S. P., Ainsworth, E. A., Rogers, A., & Ort, D. R. (2004). Rising atmospheric carbon dioxide: Plants FACE the future. *Annual Review Plant Biology*, *55*, 591–628. https://doi.org/10.1146/annurev.arplant.55.031903.141610

Loriaux, S. D., Avenson, T. J., Wells, J. M., McDermitt, D. K., Eckles, R. D., Riensche, B., & Genty, B. (2013). Closing in on maximum yield of chlorophyll fluorescence using a single multiphase flash of sub-saturating intensity. *Plant Cell and Environment*, *36*, 1755–1770. https://doi.org/10.1111/pce.2013.36.issue-10

Luo, H. B., Ma, L., Xi, H. F., Duan, W., Li, S. H., Loescher, W., … Wang, L. J. (2011). Photosynthetic responses to heat treatments at different temperatures and following recovery in grapevine (*Vitis amurensis* L.) leaves. *PLoS ONE*, *6*, e23033. https://doi.org/10.1371/journal.pone.0023033

Luo, Y., Su, B., Currie, W. S., Dukes, J. S., Finzi, A., Hartwig, U., … Field, C. B. (2004). Progressive nitrogen limitation of ecosystem responses to rising atmospheric carbon dioxide. *BioScience*, *54*, 731–739. https://doi.org/10.1641/0006-3568(2004)054[0731:PNLOER]2.0.CO;2

Medlyn, B. E., Barton, C. V. M., Broadmeadow, M. S. J., Ceulemans, R., De Angelis, P., Forstreuter, M., … Jarvis, P. G. (2001). Stomatal conductance of forest species after long-term exposure to elevated CO_2 concentration: A synthesis. *New Phytologist*, *149*, 247–264. https://doi.org/10.1046/j.1469-8137.2001.00028.x

Medlyn, B. E., Dreyer, E., Ellsworth, D., Forstreuter, M., Harley, P. C., Kirschbaum, M. U. F., … Loustau, D. (2002). Temperature response of parameters of a biochemically based model of photosynthesis. II. A review of experimental data. *Plant, Cell and Environment*, *25*, 1167–1179. https://doi.org/10.1046/j.1365-3040.2002.00891.x

Medlyn, B. E., Loustau, D., & Delzon, S. (2002). Temperature response of parameters of a biochemically based model of photosynthesis. I. Seasonal changes in mature maritime pine (*Pinus pinaster Ait.*). *Plant, Cell and Environment*, *25*, 1155–1165. https://doi.org/10.1046/j.1365-3040.2002.00890.x

Müller, J., Wernecke, P., & Diepenbrock, W. (2005). LEAFC3-N: A nitrogen sensitive extension of the CO_2 and H_2O gas exchange model LEAFC3 parameterized and tested for winter wheat (*Triticum aestivum* L.). *Ecological Modelling*, *183*, 183–210. https://doi.org/10.1016/j.ecolmodel.2004.07.025

Niu, S., Li, Z., Xia, J., Han, Y., Wu, M., & Wan, S. (2008). Climatic warming changes plant photosynthesis and its temperature dependence in a temperate steppe of northern China. *Environmental and Experimental Botany*, *63*, 91–101. https://doi.org/10.1016/j.envexpbot.2007.10.016

Okada, M., Lieffering, M., Nakamura, H., Kim, H. Y., & Kobayashi, K. (2001). Free air CO_2 enrichment (FACE) using pure CO2 injection: System description. *New Phytologist*, *150*, 251–260. https://doi.org/10.1046/j.1469-8137.2001.00097.x

Onoda, Y., Hikosaka, K., & Hirose, T. (2005). The balance between RuBP carboxylation and RuBP regeneration: A mechanism underlying the interspecific variation in acclimation of photosynthesis to seasonal change in temperature. *Functional Plant Biology*, *32*, 903–910. https://doi.org/10.1071/FP05024

Peng, S., Laza, M. R. C., Garcia, F. V., & Cassman, K. G. (1995). Chlorophyll meter estimates leaf area-based nitrogen concentration of rice. *Communications in Soil Science and Plant Analysis*, *26*, 927–935. https://doi.org/10.1080/00103629509369344

Pérez, P., Morcuende, R., Martin del Molino, I., & Martinez-Carrasco, R. (2005). Diurnal changes of Rubisco in response to elevated CO_2, temperature and nitrogen in wheat grown under temperature gradient tunnels. *Environmental and Experimental Botany*, *53*, 13–27. https://doi.org/10.1016/j.envexpbot.2004.02.008

Perez-Martin, A., Flexas, J., Ribas-Carbó, M., Bota, J., Tomás, M., Infante, J. M., & Diaz-Espejo, A. (2009). Interactive effects of soil water deficit and air vapour pressure deficit on mesophyll conductance to CO_2 in *Vitis vinifera* and *Olea europaea*. *Journal of Experimental Botany*, *60*, 2391–2405. https://doi.org/10.1093/jxb/erp145

Peterson, A. G., Ball, J. T., Luo, Y., Field, C. B., Reich, P. B., Curtis, P. S., … 1 Cmeal Participants (1999). The photosynthesis-leaf nitrogen relationship at ambient and elevated atmospheric carbon dioxide: A meta-analysis. *Global Change Biology*, *5*, 331–346. https://doi.org/10.1046/j.1365-2486.1999.00234.x

Poorter, H., Niinemets, U., Poorter, L., Wright, I. J., & Villar, R. (2009). Causes and consequences of variation in leaf mass per area (LMA): A meta-analysis. *New Phytologist*, *192*, 565–588. https://doi.org/10.1111/nph.2009.182.issue-3

Pozo, A. D., Pérez, P., Morcuende, R., Alonso, A., & Martínez-Carrasco, R. (2005). Acclimatory responses of stomatal conductance and photosynthesis to elevated CO_2 and temperature in wheat crops grown at varying levels of N supply in a Mediterranean environment. *Plant Science*, *169*, 908–916. https://doi.org/10.1016/j.plantsci.2005.06.009

Rosenthal, D. M., Ruiz-Vera, U. M., Sievers, M. H., Bernacchi, C. J., Ort, D. R. (2013). Biochemical acclimation and stomatal limitation of Soybean. *In Abstracts of the 16th International Congress of photosynthesis Research*, August 11–16 (2013) . St Louis, MO, USA. https://www.dropbox.com/sh/99yhbgrraezfakg/eta5ugper8/ROSENTHALDICPR_2013.pdf.

Sage, R. F., Sharkey, T. D., & Seemann, J. R. (1989). Acclimation of photosynthesis to elevated CO_2 in five C_3 species. *Plant Physiology*, *89*, 590–596. https://doi.org/10.1104/pp.89.2.590

Sakai, H., Hasegawa, T., & Kobayashi, K. (2006). Enhancement of rice canopy carbon gain by elevated CO_2 is sensitive to growth stage and leaf nitrogen concentration. *New Phytologist*, *170*, 321–332. https://doi.org/10.1111/nph.2006.170.issue-2

Scafaro, A. P., von Caemmerer, S., Evans, J. R., & Atwell, B. J. (2011). Temperature response of mesophyll conductance in cultivated and wild *Oryza* species with contrasting mesophyll cell wall thickness. *Plant, Cell and Environment*, *34*, 1999–2008. https://doi.org/10.1111/j.1365-3040.2011.02398.x

Shimono, H., Okada, M., Inoue, M., Nakamura, H., Kobayashi, K., & Hasegawa, T. (2010). Diurnal and seasonal variations in stomatal conductance of rice at elevated atmospheric CO_2 under fully open-air conditions. *Plant, Cell and Environment*, *33*, 322–331. https://doi.org/10.1111/pce.2010.33.issue-3

Stitt, M., & Krapp, A. (1999). The interaction between elevated carbon dioxide and nitrogen nutrition: The physiological and molecular background. *Plant, Cell and Environment*, *22*, 583–621. https://doi.org/10.1046/j.1365-3040.1999.00386.x

Vialet-Chabrand, S., Dreyer, E., & Brendel, O. (2013). Performance of a new dynamic model for predicting diurnal time courses of stomatal conductance at the leaf level. *Plant, Cell and Environment*, *36*, 1529–1546. https://doi.org/10.1111/pce.2013.36.issue-8

von Caemmerer, S. (2000). *Biochemical models of leaf photosynthesis*. Canberra, ACT: CSIRO Publishing.

von Caemmerer, S., & Evans, J. R. (1991). Determination of the average partial pressure of CO_2 in chloroplasts from leaves of several C_3 plants. *Australian Journal of Plant Physiology*, *18*, 287–305. https://doi.org/10.1071/PP9910287

von Caemmerer, S., & Evans, J. R. (2015). Temperature responses of mesophyll conductance differ greatly between species. *Plant, Cell and Environment*, *38*, 629–637. https://doi.org/10.1111/pce.2015.38.issue-4

von Caemmerer, S., Farquhar, G., & Berry, J. (2009). Biochemical model of C_3 photosynthesis. In A. Lasik, L. Nebal, & Govindjee (Eds.), *Photosynthesis in silico: Understanding complexity from molecules to ecosystems* (pp. 209–230). Dordrecht, The Netherlands: Springer Science+Business Media B.V. https://doi.org/10.1007/978-1-4020-9237-4

Warren, C. R. (2004). The photosynthetic limitation posed by internal conductance to CO_2 movement is increased by nutrient supply. *Journal of Experimental Botany*, *55*, 2313–2321. https://doi.org/10.1093/jxb/erh239

Way, D., & Sage, R. (2008). Thermal acclimation of photosynthesis in black spruce [*Picea mariana* (Mill.) B.S.P.]. *Plant, Cell and Environment*, *31*, 1250–1262. https://doi.org/10.1111/pce.2008.31.issue-9

Yamaguchi, D. P., Nakaji, T., Hiura, T., & Hikosaka, K. (2016). Effects of seasonal change and experimental warming on the temperature dependence of photosynthesis in the canopy leaves of *Quercus serrate*. *Tree Physiology*, *00*, 1–13.

Yamori, W., Noguchi, K., Hanba, Y. T., & Terashima, I. (2006). Effects of internal conductance on the temperature dependence of the photosynthetic rate in spinach leaves from contrasting growth temperatures. *Plant Cell Physiology*, *47*, 1069–1080. https://doi.org/10.1093/pcp/pcj077

Yamori, W., Noguchi, K., & Terashima, I. (2005). Temperature acclimation of photosynthesis in spinach leaves: Analyses of photosynthetic components and temperature dependencies of photosynthetic partial reactions. *Plant, Cell and Environment*, *28*, 536–547. https://doi.org/10.1111/pce.2005.28.issue-4

Yin, X. (2013). Improving ecophysiological simulation models to predict the impact of elevated atmospheric CO_2 concentration on crop productivity. *Annals of Botany*, *112*, 465–475. https://doi.org/10.1093/aob/mct016

Yin, X., & Struik, P. C. (2009a). C_3 and C_4 photosynthesis models: An overview from the perspective of crop modelling. *NJAS-Wageningen Journal of Life Science*, *57*, 27–38. https://doi.org/10.1016/j.njas.2009.07.001

Yin, X., & Struik, P. C. (2009b). Theoretical reconsiderations when estimating the mesophyll conductance to CO_2 diffusion in leaves of C_3 plants by analysis of combined gas exchange and chlorophyll fluorescence measurements. *Plant*, *Cell and Environment*, *32*, 1513–1524 (with corrigendum in PC&E **33,** 1595). https://doi.org/10.1111/pce.2009.32.issue-11

Yin, X., & Struik, P. C. (2015). Constraints to the potential efficiency of converting solar radiation into phytoenergy in annual crops: From leaf biochemistry to canopy physiology and crop ecology. *Journal of Experimental Botany*, *66*, 6535–6549. https://doi.org/10.1093/jxb/erv371

Yin, X., Struik, P. C., Romero, P., Harbinson, J., Evers, J. B., van den Putten, P. E. L., & Vos, J. (2009). Using combined measurements of gas exchange and chlorophyll fluorescence to estimate parameters of a biochemical C_3 photosynthesis model: A critical appraisal and a new integrated approach applied to leaves in a wheat (*Triticum aestivum*) canopy. *Plant, Cell and Environment*, *32*, 448–464. https://doi.org/10.1111/pce.2009.32.issue-5

Yin, X., Sun, Z., Struik, P. C., & Gu, J. (2011). Evaluating a new method to estimate the rate of leaf respiration in the light by analysis of combined gas exchange and chlorophyll fluorescence measurements. *Journal of Experimental Botany*, *62*, 3489–3499. https://doi.org/10.1093/jxb/err038

Yin, X., van der Putten, P. E. L., Driever, S. M., & Struik, P. C. (2016). Temperature response of bundle-sheath conductance in maize leaves. *Journal of Experimental Botany*, *67*, 2699–2714. https://doi.org/10.1093/jxb/erw104

Yoshimoto, M., Oue, H., & Kobayashi, K. (2005). Energy balance and water use efficiency of rice canopies under free-air CO_2 enrichment. *Agricultural and Forest Meteorology*, *133*, 226–246. https://doi.org/10.1016/j.agrformet.2005.09.010

Zhang, N., Li, G., Yu, S., An, D., Sun, Q., Weihong, L., & Yin, X. (2017). Can the responses of photosynthesis and stomatal conductance to water and nitrogen stress combinations be modelled using a single set of parameters? *Frontiers in Plant Science*, *8*, 323. https://doi.org/10.3389/fpls2017.00328

Zhu, G., Li, X., Su, Y., Lu, L., & Huang, C. (2011). Seasonal fluctuations and temperature dependence in photosynthetic parameters and stomatal conductance at the leaf scale of *Populus euphratica* Oliv. *Tree Physiology*, *31*, 178–195. https://doi.org/10.1093/treephys/tpr005

Zhu, C., Ziska, L., Zhu, J., Zeng, Q., Xie, Z., Tang, H., … Hasegawa, T. (2012). The temporal and species dynamics of photosynthetic acclimation in flag leaves of rice (*Oryza sativa*) and wheat (*Triticum aestivum*) under elevated carbon dioxide. *Physiologia Plantarum*, *145*, 395–405. https://doi.org/10.1111/ppl.2012.145.issue-3

SUPPORTING INFORMATION

Additional Supporting Information may be found online in the supporting information tab for this article.

How to cite this article: Cai C, Li G, Yang H, et al. Do all leaf photosynthesis parameters of rice acclimate to elevated CO_2, elevated temperature, and their combination, in FACE environments? *Glob Change Biol*. 2018;24:1685–1707. https://doi.org/10.1111/gcb.13961